

Los Alamos

NATIONAL LABORATORY

memorandum

Los Alamos Neutron Science Center, LANSCE-1
Accelerator Physics and Engineering Group

To: Distribution
From: Barbara Blind, LANSCE-1, H808
Phone/Fax: 5-2607/5-2904
Symbol: LANSCE-1:99-173
Date: September 15, 1999
Email: bblind@lanl.gov

SUBJECT: SNS CCDTL and CCL Beam-Steering Issues

Introduction

This memo addresses three issues related to beam steering in the SNS CCDTL and CCL.

One issue concerns the use of extra windings in the quadrupoles to generate the dipole fields needed to steer the beam. This approach entails substantial systematic sextupole fields, which might be expected to pose a problem. However, it could be shown that little effect on the beam will result from the sextupole fields, at least for machines with the nominal alignment tolerances. However, for machines with looser alignment tolerances the beam quality will be compromised by the sextupole fields. Machines with four times the nominal alignment tolerances will see a pronounced effect due to the sextupole fields, but will also experience beam losses due to the large beam-centroid excursions. In other words, it is unlikely that we would operate such a machine without first taking some corrective actions.

The second issue concerns the steerer spacings. Initially, a complete steering unit, consisting of two horizontal steerers, two vertical steerers and two BPMs, was assumed to be located with 11-quadrupole spacings. The steering scheme with the initial 11-quadrupole spacings had been optimized for an earlier machine with larger values for the transverse phase advances. It was compared to steering schemes with 17-quadrupole and 34-quadrupole spacings that were tailored specifically to the machine with the present transverse phase advances. It is obvious by comparing the steering scheme with the initial 11-quadrupole spacing to those with 17-quadrupole and 34-quadrupole spacings, that judicious placement of the components of each steering unit has a larger effect on the steerer strengths than different spacings between the steering units. Obviously, a machine with optimally placed components at one tune will not have optimally placed components at a significantly different tune. One should keep this in mind when advertising a machine that can run at a wide range of tunes.

The third issue concerns the BPM tolerances. It could be shown that one should strive to achieve the present nominal tolerances.

I will briefly review the nominal error limits for the beamline elements, with particular emphasis on the alignment errors, and the nominal rms errors of the BPMs. I will then define the steering scheme with the initial 11-quadrupole spacings, as well as the steering schemes with 17-quadrupole and 34-quadrupole spacings. I will also quantify the systematic sextupole field associated with a dipole field generated with extra windings in a

quadrupole. Following this introductory work, I will present the results of a number of simulations.

Nominal Error Limits for Beamline Elements and Nominal rms Errors of BPMs

Except as mentioned below, the LINAC simulations were performed with the nominal error limits shown in Table 1a. Based on the random number assigned to a beamline element during a particular run, and the error limit e , an actual error with a value in the range between $-e$ and $+e$ is chosen. The values are uniformly distributed between $-e$ and $+e$.

Table 1a. Nominal error limits for beamline elements of SNS CCDTL and CCL.

name of parameter	description of error	limit on error
EQD	quadrupole transverse displacement	0.0127 cm (5.0 mil)
EQT	quadrupole tilt	10.0 mrad
EQR	quadrupole roll	5.0 mrad
EQS	quadrupole-gradient error	0.25%
EDBC	error in distance between end gaps of adjacent segments	0.0254 cm (10.0 mil)
ECAVL	error in distance between adjacent gaps of a segment	0.00508 cm (2.0 mil)
ESD	segment transverse displacement	0.0508 cm, at ends (a)
EFM	module field-amplitude error (dynamic)	0.5%
EPHM	module phase error (dynamic)	0.5°
EFSET	module field-amplitude error (static)	1.0%
EPSET	module phase error (static)	1.0°
EFS	segment field-amplitude error (static)	1.0%
EFTILT	field-amplitude tilt in module	1.0%, at ends (b)

(a) independent misalignments of the two ends, resulting in displacements and tilts

(b) low at one end and high at other end, or vice versa

The nominal error limits are also shown in Appendix A. Appendix A is a listing of the first of ten linac.inp files used for a set of runs. The only differences between the ten linac.inp files are the random-number seeds iseedsta and iseeddyn. The listing also shows other information transparent to those familiar with running LINAC.

The main contributors to steering the beam off axis are transverse quadrupole displacements and, to a lesser degree, transverse segment (defined as accelerating structure between quadrupoles) displacements. Thus, the error limits worth pointing out are a transverse quadrupole alignment to 5 mil (EQD=0.0127 cm) and a transverse segment alignment to 20 mil (ESD=-0.0508 cm). The minus sign means that the two ends of a segment are independently aligned, leading to displacements and tilts.

The nominal rms errors for the readings of the three types of BPMs are given in Table 1b. The BPM errors depend on the BPM radius. For the 1.50-cm-radius BPMs, the nominal

rms error is 0.021 cm, for the 1.75-cm-radius BPMs it is 0.023 cm, and for the 2.00-cm-radius BPMs it is 0.024 cm. In LINAC notation, pmtol(1)=128*0.021, 49*0.023, 168*0.024, as shown in Appendix A.

Table 1b. Nominal rms errors for readings of three types of BPMs.

name of parameter	description of error	limit on error
PMTOL(1-128)	reading of 1.50-cm-radius BPM	0.021 cm
PMTOL(129-177)	reading of 1.75-cm-radius BPM	0.023 cm
PMTOL(177-345)	reading of 2.00-cm-radius BPM	0.024 cm

Unlike the other errors, which are uniformly distributed, the BPM errors have Gaussian distributions truncated at 3σ .

Beam steering is simulated by bringing the beam centroid back to the axis, at the two BPMs of each steering unit, with the appropriate horizontal and vertical deflections of the four steerers of the steering unit. When the BPM errors are turned off, the beam centroid is brought exactly to the axis. For nonzero PMTOL values, the beam centroid is off axis by distances that are computed from the random numbers chosen for each BPM and the rms error of the BPM.

Steering Scheme with Initial 11-Quadrupole Spacings

A steering unit consists of two horizontal steerers, two vertical steerers and two BPMs. The horizontal steerers should be in horizontally focusing quadrupoles and the vertical steerers should be in horizontally defocusing quadrupoles.

The code LINAC defines a cell as a quadrupole followed by an accelerating structure. Thus, the CCDTL starts with a quadrupole, Q1, which happens to be a horizontally defocusing quadrupole. When Ken Crandall first set up the steering scheme, the transverse phase advance per cell was 60° at the end of the CCL and larger in the earlier cells. Steerers were located in adjacent quadrupoles. The first steering unit started in quadrupole Q4. Thus, there were horizontal steerers in Q4 and Q6, vertical steerers in Q5 and Q7, and BPMs in Q7 and Q9. In LINAC notation, the steerer locations are specified as itsm(4,1)=1,2,1,2, where a “1” represents horizontal steering and a “2” represents vertical steering. The BPM locations are specified as itpm(4,1)=3,0,3, where a “3” means a position measurement in both planes and a “0” means no position measurement. The pattern was repeated with 11-quadrupole spacings, with the next set of steerers in Q15 through Q18 and BPMs in Q18 and Q20, or itsm(15,1)=2,1,2,1, itpm(18,1)=3,0,3.

In the early studies, when the CCDTL had a 1.25-cm aperture, we noticed some beam scraping at the start of the CCDTL due to the beam-centroid displacement at the entrance to the CCDTL. This displacement was caused by the alignment errors, but lack of steering, in the DTL. The problem was alleviated by moving the first steering unit upstream. Actually, we moved the first six steering units upstream. Thus, most error studies were performed with steerers in Q1 through Q4, BPMs in Q4 and Q6, steerers in Q12 through Q15, BPMs in Q15 and Q17, and so forth, and then steerers in Q70 through

Q73 and BPMs in Q73 and Q75, and so forth. This steering scheme is shown in Appendix A.

The latest accelerator tune ends with 40° phase advance per cell, and we even briefly studied a machine that ended with 30° phase advance per cell. However, we never adjusted the steerer configuration. The configuration of Appendix A is referred to as the steering scheme with the initial 11-quadrupole spacings. This name is supposed to imply that a better configuration with 11-quadrupole spacings exists.

Steering Scheme with 17-Quadrupole Spacings

In June, we discovered a disconnect between the beam-optics assumption about the number of steerers and BPMs, and the assumption of the diagnostics team about the same quantities.

The diagnostics team had assumed horizontal steerer pairs with 34-quadrupole spacings and vertical steerer pairs with 34-quadrupole spacings, interlaced in such a way that there were BPM pairs with 17-quadrupole spacings.

I first reduced the number of BPMs to what had been assumed by the diagnostics team. However, I kept two horizontal and two vertical steerers with each set of BPMs.

Keeping in mind that the ideal phase advance between steerers is 90°, and the ideal phase advance between BPMs is 90°, I adjusted the layout of the steering units in the latter part of the machine, where the transverse phase advance per cell ramps down to 40°. There were no layout changes for the first four steering units. The description of the steering scheme with 17-quadrupole spacings is given in Appendix B.

Steering Scheme with 34-Quadrupole Spacings

I also studied a steering scheme where the number of steerers is as assumed by the diagnostics team. However, the horizontal and vertical steerers did not alternate. Instead, the steering scheme was arrived at by simply removing every other steering unit, and thus the number of BPMs is half that assumed by the diagnostics team. Details about the steering scheme with 34-quadrupole spacings are presented in Appendix C.

Effect of Systematic Sextupole Fields of Steerers

The steering can be accomplished with dipole magnets, with a realignment of the quadrupoles or with extra windings in the quadrupoles.

When a dipole field $B_{y,d}$ is generated with extra windings in a quadrupole, this also causes a sextupole field B_s , where

$$B_{y,s}(y=0) = B_{y,d} \frac{P}{4} \left(\frac{x}{r} \right)^2.$$

The sextupole field amounts to 44.2% of the dipole field at 75% of the aperture radius r . The formula was derived by Peter Walstrom. It is in good agreement with data from simulations performed by Ted Hunter, from which I had computed 44.8% sextupole at 75% of the aperture radius.

For the simulations, I used two versions of the LINAC code, one where sextupole fields of 45% of the dipole fields, at 75% of the aperture radius, are assumed and one where sextupole fields of 0.0% of the dipole fields are assumed.

The study of the effect of the sextupole fields of the steerers was conducted by running the same ten machines without and with these fields. In each case, four plots were produced, namely a plot of the transverse and longitudinal rms emittances, a plot of the maximum transverse beam extents, a plot of the transverse beam-centroid positions along the accelerators and a plot of the steerer strengths required to properly steer the beam through the ten machines. In all cases, the BPMs had the nominal rms errors. The cases without sextupole fields are shown in the top plots and the cases with sextupole fields are shown in the bottom plots of Figures 1 through 20.

Figures 1 through 4 represent the steering scheme with the initial 11-quadrupole spacings. Figure 1 shows the transverse and longitudinal rms emittances. They are very similar for the machines without sextupoles and the machines with sextupoles, with the transverse rms emittances being very slightly larger for the machines with sextupoles.

The minimum transverse rms emittance $\epsilon_{t,\min}$, maximum transverse rms emittance $\epsilon_{t,\max}$, minimum longitudinal rms emittance $\epsilon_{l,\min}$, and maximum longitudinal rms emittance $\epsilon_{l,\max}$ for the ten runs are given in Table 2.

Table 2. Lower and upper limits of transverse rms emittances ($\epsilon_{t,\min}$, $\epsilon_{t,\max}$) and longitudinal rms emittances ($\epsilon_{l,\min}$, $\epsilon_{l,\max}$). Each case is described by (a) steering-unit spacings (initial 11-quadrupole, 17-quadrupole, or 34-quadrupole spacings), (b) presence of sextupole fields (yes or no), (c) BPM errors (with 1X meaning nominal), and (d) Figure numbers representing the case.

(a)	(b)	(c)	(d)	$\epsilon_{t,\min}$ [π -cm-mrad]	$\epsilon_{t,\max}$ [π -cm-mrad]	$\epsilon_{l,\min}$ [π -cm-mrad]	$\epsilon_{l,\max}$ [π -cm-mrad]
11	no	1X	1 – 4	0.0321	0.0399	0.0497	0.0668
11	yes	1X	1 – 4	0.0325	0.0400	0.0496	0.0658
17	no	1X	5 – 8	0.0319	0.0435	0.0488	0.0821
17	yes	1X	5 – 8	0.0326	0.0434	0.0487	0.0817
34	no	1X	9 – 12	0.0323	0.0418	0.0478	0.0662
34	yes	1X	9 – 12	0.0325	0.0424	0.0480	0.0653
17	no	2X	13 – 16	0.0332	0.0478	0.0524	0.0844
17	yes	2X	13 – 16	0.0334	0.0510	0.0520	0.0848
17	no	4X	17 – 20	0.0353	0.1135	0.0557	0.0874
17	yes	4X	17 – 20	0.0375	0.0698	0.0562	0.0833

Figure 2 shows the maximum beam extents. They, too, are very similar for the two sets of runs. Thus, for the steering scheme with the initial 11-quadrupole spacings, and the nominal 5-mil transverse quadrupole displacements and 20-mil transverse segment displacements, I found the effect of the sextupole fields on the beam to be negligible.

Figure 3 shows the beam centroids. They should not depend on the sextupole content of the steerers and, indeed, they do not. Figure 4 shows the steerer strengths required to bring the beam to positions near the axis, at the BPMs. These should also not depend on the sextupole content of the steerers, as is obvious from inspection of Figure 4. The largest steerer strength required is 2853 G-cm. The steerer strengths increase along the machine, because of increasing beam rigidity, and a less-than-optimal steerer arrangement especially in the high-energy end of the machine.

Figures 5 through 8 correspond to Figures 1 through 4, but for the steering scheme with the 17-quadrupole spacings. Just like for Figure 1, the minimum transverse rms emittance is slightly larger with the sextupoles as compared to without the sextupoles, but this is certainly not a pronounced effect (see Table 2). However, Figure 1 shows smaller transverse rms emittances as well as smaller longitudinal rms emittances than Figure 5. This could be interpreted to mean that the beam quality is compromised by going to the larger spacings, maybe because the beam goes further off axis and thus encounters more nonlinearities from cavity fields and quadrupole fringe fields.

Figure 6 shows very similar maximum beam extents for the two sets of runs. The top and bottom plots of Figure 7, and Figure 8, are again identical. Figure 7, compared to Figure 3, shows somewhat smaller beam-centroid excursions. This might be explained by the fact that the steering is more successful when the components of the steering units are at near-ideal locations. On the other hand, the beam-quality deterioration for the steering scheme with the 17-quadrupole spacings compared to the steering scheme with the initial 11-quadrupole spacings is no longer transparent. The actual explanation is as follows. When the BPM errors are turned on, they require random numbers and thus in one case machines with ten sets of errors were studied and in the other case machines with ten different sets of errors were considered.

Figure 8, compared to Figure 4, shows that the required steerer strengths are significantly reduced when the steerers are optimally placed, even though there are fewer of them and thus they should otherwise need to be stronger. The maximum steerer strength in the part of the machine where the spacings between steerers had been increased to near 90° phase advance is 1267 G-cm, compared to a value of 2853 G-cm for the steering scheme with the initial 11-quadrupole spacings. The largest steerer strength in any of the steering units (except for the first steering unit, which in all cases simply compensates for the DTL errors) is 1567 G-cm.

Figures 9 through 12 correspond to Figures 5 through 8, but for the steering scheme with the 34-quadrupole spacings. Figure 9 again shows slightly larger transverse rms emittances for steerers with sextupole fields as compared to steerers without sextupole fields. This is also shown in Table 2. The machine with the very large longitudinal rms emittance present in Figure 5 is not present in Figure 9. Also, the largest transverse rms emittances of Figure 9 are smaller than those of Figure 5.

The top and bottom plots of Figure 10 again are very similar and the top and bottom plots of Figures 11 and 12 are identical.

Figure 11, compared to Figure 7, shows that for the steering scheme with the 34-quadrupole spacings the beam centroid can get about twice as far off axis as for the

steering scheme with the 17-quadrupole spacings, as would be expected. Similarly, Figure 12, compared to Figure 8, shows that larger steerer strengths are required to restore the beams to the axis. The largest steerer strength in the latter part of the machine is 1654 G-cm, compared to 1267 G-cm. Neglecting the first steering unit, the steerer strengths along the machine are up to 1654 G-cm, compared to 1567 G-cm. Also, Figure 10 shows maximum beam extents that are slightly larger than those of Figure 6.

Thus, within the parameters where we intend to operate, the sextupole fields of the steerers do not seem to pose a problem. To see if this would still be true when more steering is required, the steering scheme with the 17-quadrupole spacings was reinvestigated with twice the limits on the errors that steer the beam off axis, namely the transverse quadrupole displacement EQD and the transverse segment displacement ESD. Nominally, these parameters are 0.0127 cm and 0.0508 cm, respectively. Thus, they were raised to 0.0254 cm and 0.1016 cm, respectively. This case is presented in Figures 13 through 17. Figures 13 through 17 should be compared to Figures 5 through 8. The sets of machines have the same errors, except for factors of two in the above-mentioned quantities.

The rms emittances are slightly increased for Figure 13, compared to Figure 5. Also, there is a slight increase from the runs without sextupoles to the runs with sextupoles (see Table 2). The maximum extents of Figure 14 are somewhat larger for the with-sextupoles runs compared to the without-sextupoles runs. The centroid excursions of Figure 15 are about twice those of Figure 7, as would be expected. In fact, the beam gets so far off axis that in one case one particle is scraped on the 1.5-cm aperture. This is not an effect of the sextupole fields, as it happens for the machine without sextupoles and the machine with sextupoles. The steerer strengths of Figure 16 likewise are about twice those of Figure 8. The largest steerer strength in the latter part of the machine is 2180 G-cm, compared to 1267 G-cm. The largest steerer strengths, excluding the first steering unit, are 2814 G-cm and 1567 G-cm, respectively.

To further increase the effect due to the sextupole fields, EQD and ESD were doubled again, to 0.0508 cm and 0.2032 cm, respectively. The results are shown in Figures 17 through 20.

In Figure 17, there is a clear difference between the runs without and the runs with sextupoles. Without sextupoles, there is more of a spread in the rms emittances. Sextupoles should couple the transverse planes, but the coupling seems to even extend to the longitudinal plane (see Table 2). There is a clear increase in the rms emittances in Figure 17, compared to Figure 5. Thus, the sextupole fields of the steerers start to affect the beam when large steerer strengths are required and the beam centroid is far off axis, due to the large misalignments.

In Figure 18, the bottom plot (with sextupoles) has larger maximum extents than the top plot (without sextupoles). Figure 19 shows that the beam-centroid excursions are about four times as large as with the nominal alignment tolerances of Figure 7.

The much increased maximum extents of the beams of Figure 18, compared to those of Figure 6, are largely due to the increased beam-centroid excursions. For the ten machines without sextupoles, 4, 17, 1, 42, 0, 0, 2, 0, 0, 0, particles, respectively, are scraped and for the ten machines with sextupoles, 3, 5, 2, 41, 0, 1, 7, 0, 1, 0, particles, respectively are

scraped. Thus, the scraping is not due to an adverse effect of the sextupole fields but due to the large excursions of the beam centroid.

Figure 20 has about four times larger steerer strengths than Figure 8, namely (excluding the first steering unit) up to 5300 G-cm versus up to 1567 G-cm.

Comparison of the Three Steering Schemes

The simulations described so far compared machines without and machines with sextupole fields in the steerers. Because of the different assignment of the random numbers for machines with different numbers of BPMs, machines with different steering schemes had different sets of errors.

To compare the steering scheme with the initial 11-quadrupole spacings to those with the 17-quadrupole and 34-quadrupole spacings, I followed Ken Crandall's suggestion and left out the errors in the BPMs. In other words, I removed the line `pmtol(1)=128*0.021, 49*0.023, 168*0.024` from the `linac.inp` files. In all cases, the machines had steerers with sextupole fields. The steering scheme with the initial 11-quadrupole spacings is represented by Figures 21 through 24, the steering scheme with the 17-quadrupole spacings is represented by Figures 25 through 28, and the steering scheme with the 34-quadrupole spacings is represented by Figures 29 through 32.

The minimum and maximum transverse and longitudinal rms emittances for the three cases are given in Table 3.

Table 3. Lower and upper limits of transverse rms emittances ($\epsilon_{t,\min}$, $\epsilon_{t,\max}$) and longitudinal rms emittances ($\epsilon_{l,\min}$, $\epsilon_{l,\max}$). Each case is described by (a) steering-unit spacings (initial 11-quadrupole, 17-quadrupole, or 34-quadrupole spacings), (b) presence of sextupole fields (yes), (c) BPM errors (with 0X meaning errors turned off), and (d) Figure numbers representing the case.

(a)	(b)	(c)	(d)	$\epsilon_{t,\min}$ [π -cm-mrad]	$\epsilon_{t,\max}$ [π -cm-mrad]	$\epsilon_{l,\min}$ [π -cm-mrad]	$\epsilon_{l,\max}$ [π -cm-mrad]
11	yes	0X	21 – 24	0.0321	0.0399	0.0448	0.0795
17	yes	0X	25 – 28	0.0314	0.0397	0.0450	0.0778
34	yes	0X	29 – 32	0.0328	0.0414	0.0452	0.0768

The steering scheme with the 17-quadrupole spacings has the smallest rms emittances. Comparison of Figures 21, 25, and 29 shows little difference between the rms emittances for the three cases. The same is true for the maximum beam extents of Figures 22, 26, and 30. The beam-centroid excursions of Figures 23 and 27 are comparable, even though the beam is brought to the axis more frequently in one case as compared to the other. The beam-centroid excursions of Figure 31 are almost twice as large as those of Figure 27.

The steerer strengths of Figure 24 are comparable to those of Figure 28. The steerer strengths of Figure 32 are somewhat larger than those of Figure 28. Neglecting the first steering unit, which corrects for the errors in the DTL, the maximum steerer strengths for the three sets of runs are 1106 G-cm, 1021 G-cm and 1571 G-cm, respectively.

Of course both the beam-centroid excursions and the steerer strengths will go up when there are BPM errors. Without BPM errors, both the steering scheme with the 17-quadrupole spacings and the steering scheme with the 34-quadrupole spacings have acceptably small steerer strengths (below about 2000 G-cm). However, one would probably not like to see the beam-centroid excursions of over 2.0 mm associated with the steering scheme with the 34-quadrupole spacings. For the steering scheme with the 17-quadrupole spacings, the beam-centroid excursions are around 1.0 mm.

Dependence on BPM Errors

Only the steering scheme with the 17-quadrupole spacings was investigated here, since it is the one adopted for the machine, albeit not precisely as simulated here.

In order to keep the same random-number sequence, the BPM errors were not turned off by removing the line $\text{pmtol}(1)=128*0.021,49*0.023,168*0.024$ when studying the case without BPM errors. Instead, the rms errors were set to very small numbers, namely $\text{pmtol}(1)=128*0.000021,49*0.000023,168*0.000024$. This was then compared to the case with the nominal BPM rms errors, $\text{pmtol}(1)=128*0.021,49*0.023,168*0.024$. Also investigated was the case with twice the nominal values, $\text{pmtol}(1)=128*0.042,49*0.046,168*0.048$, and the case with three times the nominal values, $\text{pmtol}(1)=128*0.063,49*0.069,168*0.072$. In all cases, the steerers had sextupole fields.

Figures 33 through 36 represent the case with minimal BPM errors. Figures 37 through 40 represent the case with the nominal BPM errors. Figures 41 through 44 represent the case with twice the nominal BPM errors. Finally, Figures 45 through 48 represent the case with three times the nominal BPM errors.

The minimum and maximum transverse and longitudinal rms emittances for the four cases are shown in Table 4. There is little difference in the transverse rms emittances between the case with minimal and the case with nominal BPM errors. At twice the nominal BPM errors, the maximum transverse rms emittance is up 18% over the nominal, at three times the nominal BPM errors, it is up 32%. Little effect is seen on the longitudinal rms emittances, at least at the output of the CCL.

Table 4. Lower and upper limits of transverse rms emittances ($\epsilon_{t,\min}$, $\epsilon_{t,\max}$) and longitudinal rms emittances ($\epsilon_{l,\min}$, $\epsilon_{l,\max}$). Each case is described by (a) steering-unit spacings (17-quadrupole spacings), (b) presence of sextupole fields (yes), (c) BPM errors (with 1X meaning nominal), and (d) Figure numbers representing the case.

(a)	(b)	(c)	(d)	$\epsilon_{t,\min}$ [π -cm-mrad]	$\epsilon_{t,\max}$ [π -cm-mrad]	$\epsilon_{l,\min}$ [π -cm-mrad]	$\epsilon_{l,\max}$ [π -cm-mrad]
17	yes	0X	33 – 36	0.0316	0.0426	0.0483	0.0836
17	yes	1X	37 – 40	0.0326	0.0434	0.0487	0.0817
17	yes	2X	41 – 44	0.0331	0.0511	0.0503	0.0825
17	yes	3X	45 – 48	0.0336	0.0572	0.0525	0.0831

There is a large effect on the beam-centroid excursions as one loses the ability to properly center the beam because of the BPM errors. For minimal BPM errors, the beam-centroid excursions, excluding the first 50 MeV, are up to 1.5 mm. With the nominal BPM errors,

they are up to 1.7 mm, with twice and three times the nominal errors, they are up to 2.6 mm and 3.5 mm, respectively.

There is a similar increase in steerer strength. For the minimal BPM errors, the steerers, excluding those of the first steering unit, have strengths of up to 1250 G-cm. With the nominal BPM errors, the steerer strengths are up to 1567 G-cm, with twice and three times the nominal errors, they are up to 2181 G-cm and 3149 G-cm, respectively.

Thus, the beam-centroid excursions, the steerer strengths required to bring the beam to the axis, and the rms emittances of the beam all strongly depend of the rms errors of the BPMs. There is little difference in these quantities between the minimal and the nominal BPM errors. However, there are large increases in these quantities between the nominal and twice the nominal BPM errors. This suggests that the nominal rms errors are reasonable values to strive for.

Summary

In summary, with the nominal alignment tolerances the effects of systematic sextupole fields in the steerers are tolerable for all three steering schemes investigated. Thus, while the approach of dedicated steerers is cleaner, there is no particular beam-optics reason to avoid steering with extra coils in the quadrupoles. One caveat is that if the alignment is much worse than anticipated then the sextupole fields will affect the beam quality. On the other hand, such machines are also expected to experience large beam losses. We would presumably not operate a machine with such losses. Instead, we would first realign the machine.

The proposed steering scheme is that with 17-quadrupole spacings. To repeat, this steering scheme can be implemented with quadrupoles with extra windings to produce the dipole fields to steer the beam, provided the alignment is not much worse than suggested by the present tolerances. These are 5-mil tolerances for the transverse alignment of the quadrupoles and 20-mil tolerances for the transverse alignment of the segments.

An effort should be made to achieve the nominal error tolerances for the BPMs since failure to do so will impact on the required steerer strengths, magnitude of the beam-centroid excursions, and transverse rms emittances of the CCL output beam. The nominal rms errors are 0.021 cm for the 1.50-cm-radius BPMs, 0.023 cm for the 1.75-cm-radius BPMs and 0.024 cm for the 2.00-cm-radius BPMs.

Appendix A. Listing of linac.inp file for steering scheme with initial 11-quadrupole spacings.

```
345 tanks
&run nml= 1, nm2= 31, de= 50., mprnt=1,
hr(1)=54*1.50, 30*1.500, 44*1.500, 49*1.750, 168*2.000
fmod(1)=500*1., ntpm=2,52,30,17,14,13,13,12,12,12,
9,9,8,8,8,8,8,8,8,8,8,8,8,8,8,8,8,7,7,

iseedsta=31201449, iseeddyn=29039190,
eqd=.0127, eqt=10.0, eqs=.0025, eqr=5.0, esd=-0.0508,
efm=.005, ephm=0.50, efset=.01, epset=1.0, edbc=.0254,
ecavl=.00508,
efs=.01, ephs=0.0, eftilt=.01,

rmesh=1.0, zmesh=2., nr=20, nz=40, nip=0, frm=1.2, xi= 112.0
nruns= 1, lprn=0, ifringe=1, ienergy=0, isteer=1, mpoles=3,

itsm(1,1)=2,1,2,1, itpm(4,1)=3,0,3, itsm(12,1)=1,2,1,2, itpm(15,1)=3,0,3,
itsm(23,1)=2,1,2,1, itpm(26,1)=3,0,3, itsm(34,1)=1,2,1,2, itpm(37,1)=3,0,3,
itsm(45,1)=2,1,2,1, itpm(48,1)=3,0,3, itsm(56,1)=1,2,1,2, itpm(59,1)=3,0,3,
itsm(70,1)=1,2,1,2, itpm(73,1)=3,0,3, itsm(81,1)=2,1,2,1, itpm(84,1)=3,0,3,
itsm(92,1)=1,2,1,2, itpm(95,1)=3,0,3, itsm(103,1)=2,1,2,1, itpm(106,1)=3,0,3,
itsm(114,1)=1,2,1,2, itpm(117,1)=3,0,3, itsm(125,1)=2,1,2,1, itpm(128,1)=3,0,3,
itsm(136,1)=1,2,1,2, itpm(139,1)=3,0,3, itsm(147,1)=2,1,2,1, itpm(150,1)=3,0,3,
itsm(158,1)=1,2,1,2, itpm(161,1)=3,0,3, itsm(169,1)=2,1,2,1, itpm(172,1)=3,0,3,
itsm(180,1)=1,2,1,2, itpm(183,1)=3,0,3, itsm(191,1)=2,1,2,1, itpm(194,1)=3,0,3,
itsm(202,1)=1,2,1,2, itpm(205,1)=3,0,3, itsm(213,1)=2,1,2,1, itpm(216,1)=3,0,3,
itsm(224,1)=1,2,1,2, itpm(227,1)=3,0,3, itsm(235,1)=2,1,2,1, itpm(238,1)=3,0,3,
itsm(246,1)=1,2,1,2, itpm(249,1)=3,0,3, itsm(257,1)=2,1,2,1, itpm(260,1)=3,0,3,
itsm(268,1)=1,2,1,2, itpm(271,1)=3,0,3, itsm(279,1)=2,1,2,1, itpm(282,1)=3,0,3,
itsm(290,1)=1,2,1,2, itpm(293,1)=3,0,3, itsm(301,1)=2,1,2,1, itpm(304,1)=3,0,3,
itsm(312,1)=1,2,1,2, itpm(315,1)=3,0,3, itsm(323,1)=2,1,2,1, itpm(326,1)=3,0,3,
itsm(334,1)=1,2,1,2, itpm(337,1)=3,0,3,
pmtol(1)=128*.021, 49*.023, 168*.024
iout=-9, optcon(1)= 0 , 10, 2.0, 1, 40., 0., 1.0, 1 &
input to CCDTL from output of DTL
&inp nn= 2, vv =11,-65. &end
SNS CCDTL, 20 - 1000 MeV
&run iend=1 &end
```

Appendix B. Excerpt from linac.inp file for steering scheme with 17-quadrupole spacings.

```
itsm(1,1)=2,1,2,1, itpm(4,1)=3,0,3, itsm(18,1)=1,2,1,2, itpm(21,1)=3,0,3,  
itsm(35,1)=2,1,2,1, itpm(38,1)=3,0,3, itsm(52,1)=1,2,0,0,1,2, itpm(57,1)=3,0,0,0,3,  
itsm(69,1)=2,1,0,0,2,1, itpm(74,1)=3,0,0,0,3, itsm(86,1)=1,2,0,0,1,2, itpm(91,1)=3,0,0,0,3,  
itsm(103,1)=2,1,0,0,2,1, itpm(108,1)=3,0,0,0,3, itsm(120,1)=1,2,0,0,1,2, itpm(125,1)=3,0,0,0,3  
'  
itsm(137,1)=2,1,0,0,2,1, itpm(142,1)=3,0,0,0,3, itsm(154,1)=1,2,0,0,1,2, itpm(159,1)=3,0,0,0,3  
'  
itsm(171,1)=2,1,0,0,2,1, itpm(176,1)=3,0,0,0,3, itsm(188,1)=1,2,0,0,1,2, itpm(193,1)=3,0,0,0,3  
'  
itsm(205,1)=2,1,0,0,2,1, itpm(210,1)=3,0,0,0,3, itsm(222,1)=1,2,0,0,1,2, itpm(227,1)=3,0,0,0,3  
'  
itsm(239,1)=2,1,0,0,2,1, itpm(244,1)=3,0,0,0,3, itsm(256,1)=1,2,0,0,1,2, itpm(261,1)=3,0,0,0,3  
'  
itsm(273,1)=2,1,0,0,2,1, itpm(278,1)=3,0,0,0,3, itsm(290,1)=1,2,0,0,1,2, itpm(295,1)=3,0,0,0,3  
'  
itsm(307,1)=2,1,0,0,2,1, itpm(312,1)=3,0,0,0,3, itsm(324,1)=1,2,0,0,1,2, itpm(329,1)=3,0,0,0,3  
'  
itsm(335,1)=2,1,0,0,2,1, itpm(340,1)=3,0,0,0,3,
```

Appendix C. Excerpt from linac.inp file for steering scheme with 34-quadrupole spacings.

```
itsm(1,1)=2,1,2,1, itpm(4,1)=3,0,3,  
itsm(35,1)=2,1,2,1, itpm(38,1)=3,0,3,  
itsm(69,1)=2,1,0,0,2,1, itpm(74,1)=3,0,0,0,3,  
itsm(103,1)=2,1,0,0,2,1, itpm(108,1)=3,0,0,0,3,  
itsm(137,1)=2,1,0,0,2,1, itpm(142,1)=3,0,0,0,3,  
itsm(171,1)=2,1,0,0,2,1, itpm(176,1)=3,0,0,0,3,  
itsm(205,1)=2,1,0,0,2,1, itpm(210,1)=3,0,0,0,3,  
itsm(239,1)=2,1,0,0,2,1, itpm(244,1)=3,0,0,0,3,  
itsm(273,1)=2,1,0,0,2,1, itpm(278,1)=3,0,0,0,3,  
itsm(307,1)=2,1,0,0,2,1, itpm(312,1)=3,0,0,0,3,  
itsm(335,1)=2,1,0,0,2,1, itpm(340,1)=3,0,0,0,3,
```

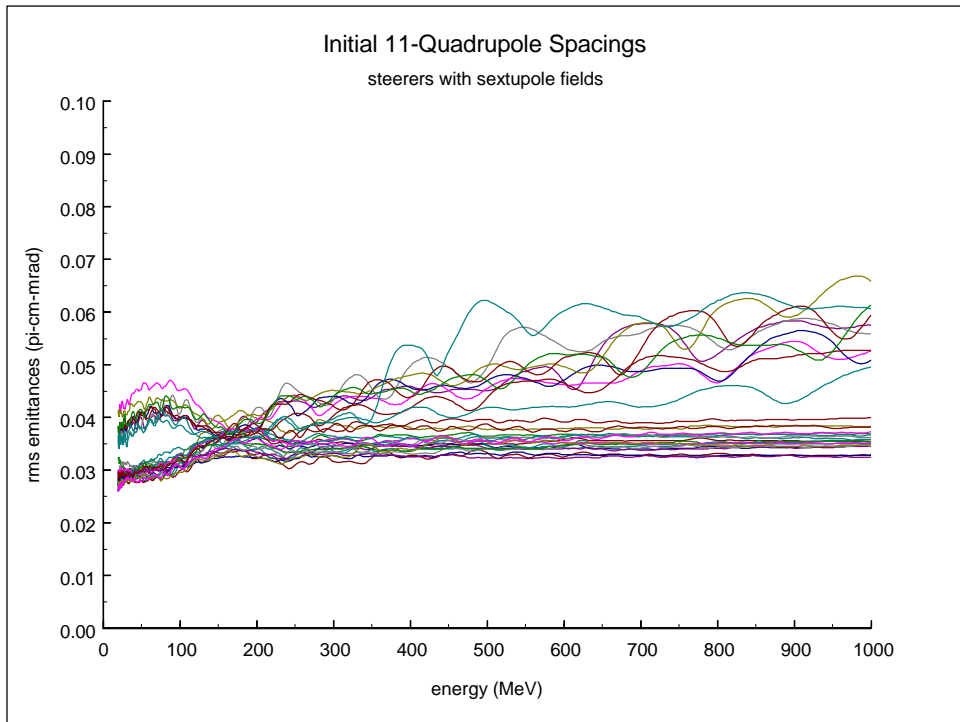
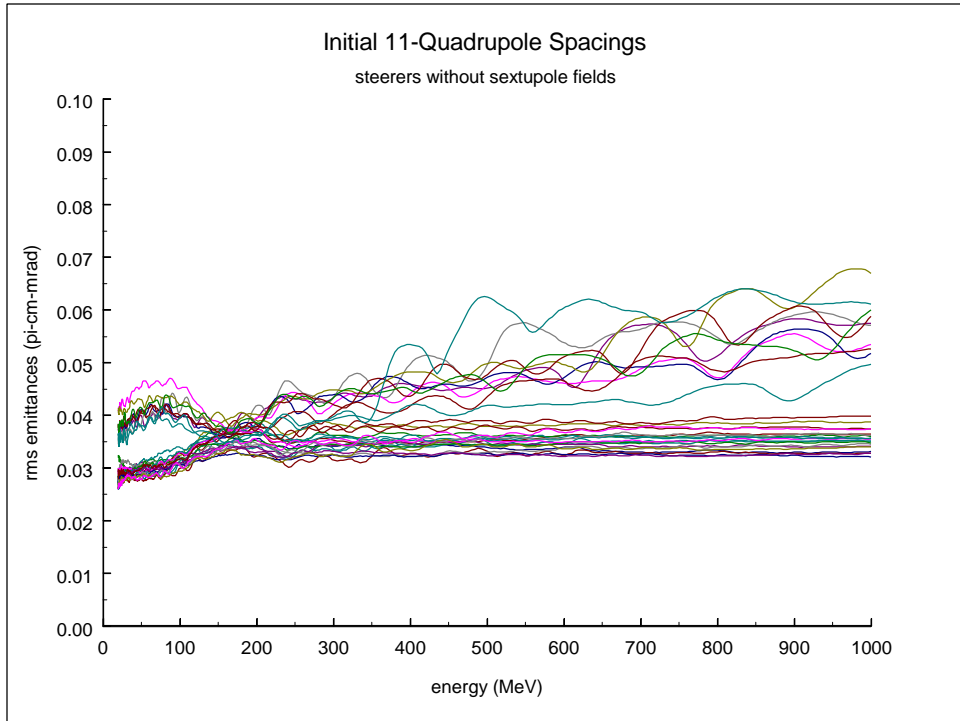


Figure 1. Transverse and longitudinal rms emittances for steering scheme with initial 11-quadrupole spacings without (top) and with (bottom) sextupole fields in steerers.

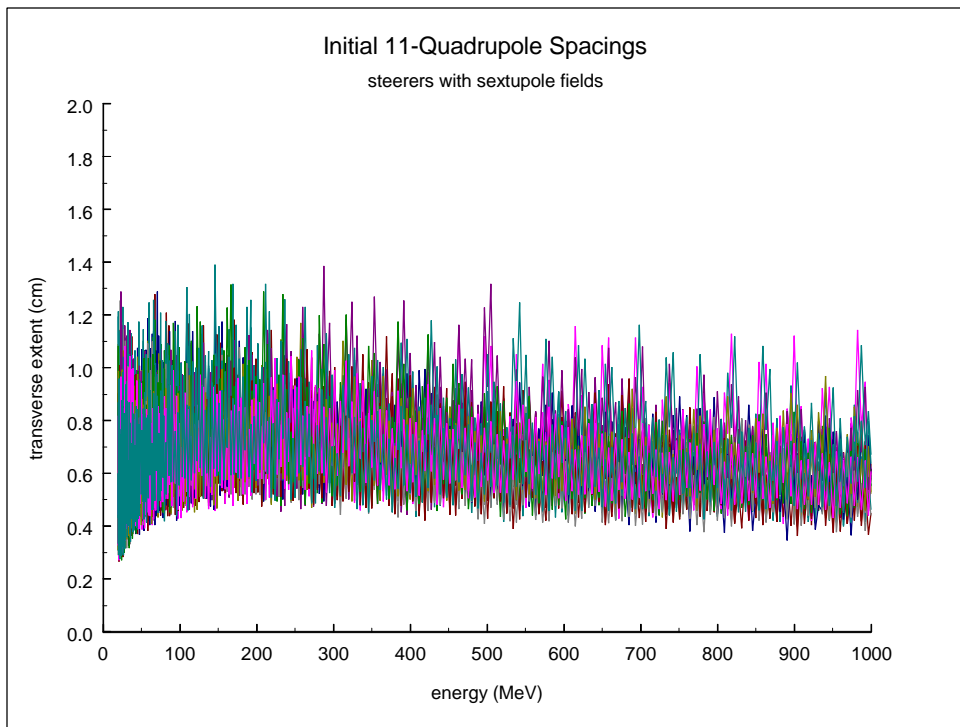
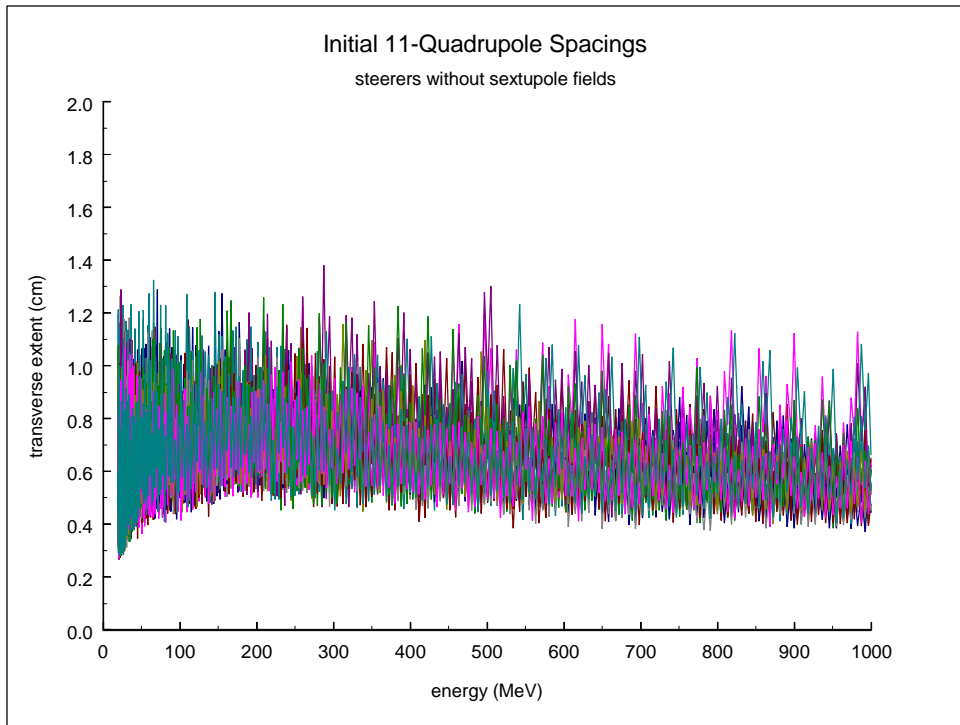


Figure 2. Maximum beam extents for steering scheme with initial 11-quadrupole spacings without (top) and with (bottom) sextupole fields in steerers.

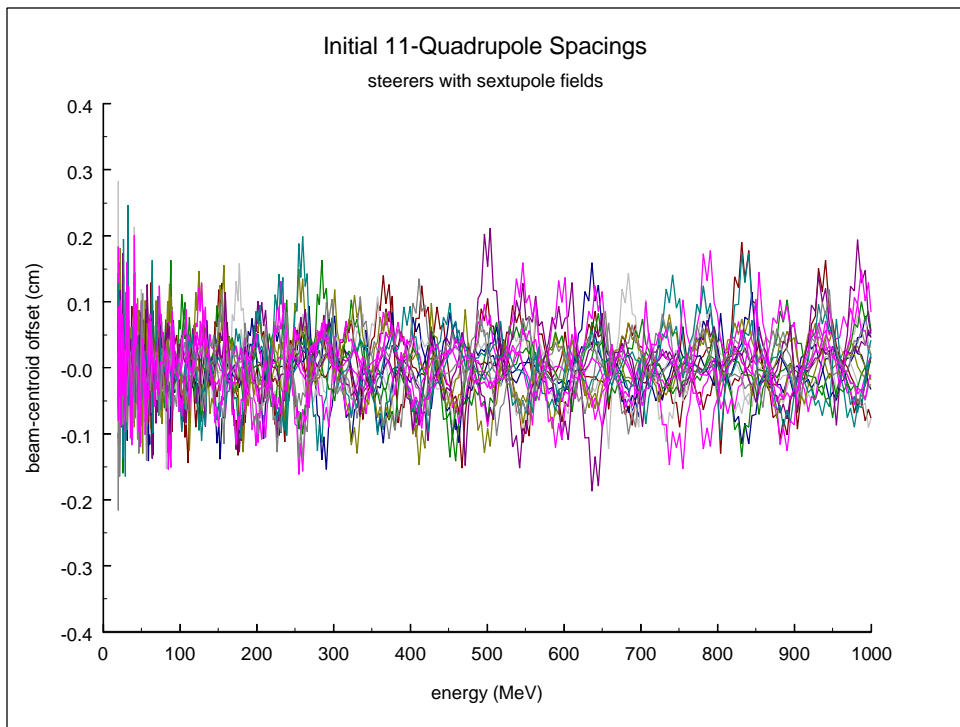
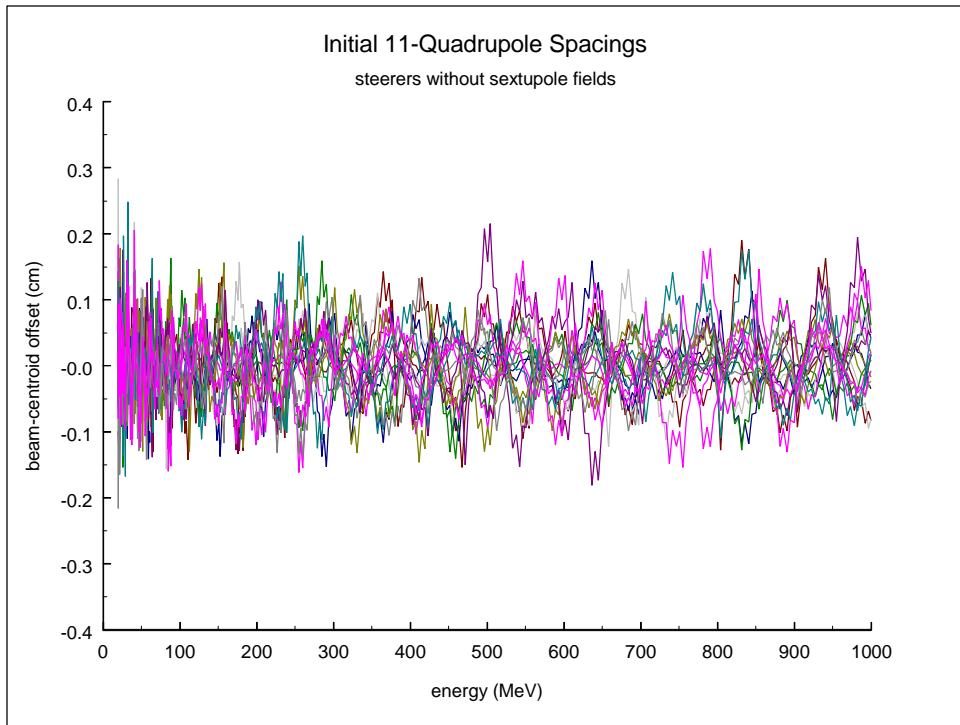


Figure 3. Beam-centroid excursions for steering scheme with initial 11-quadrupole spacings without (top) and with (bottom) sextupole fields in steerers.

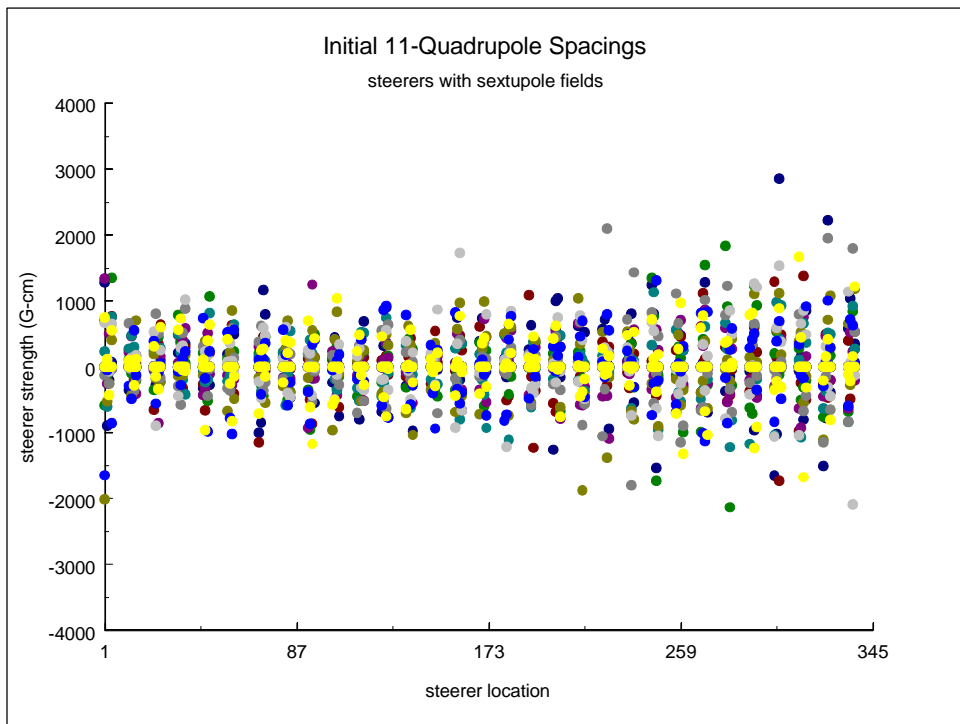
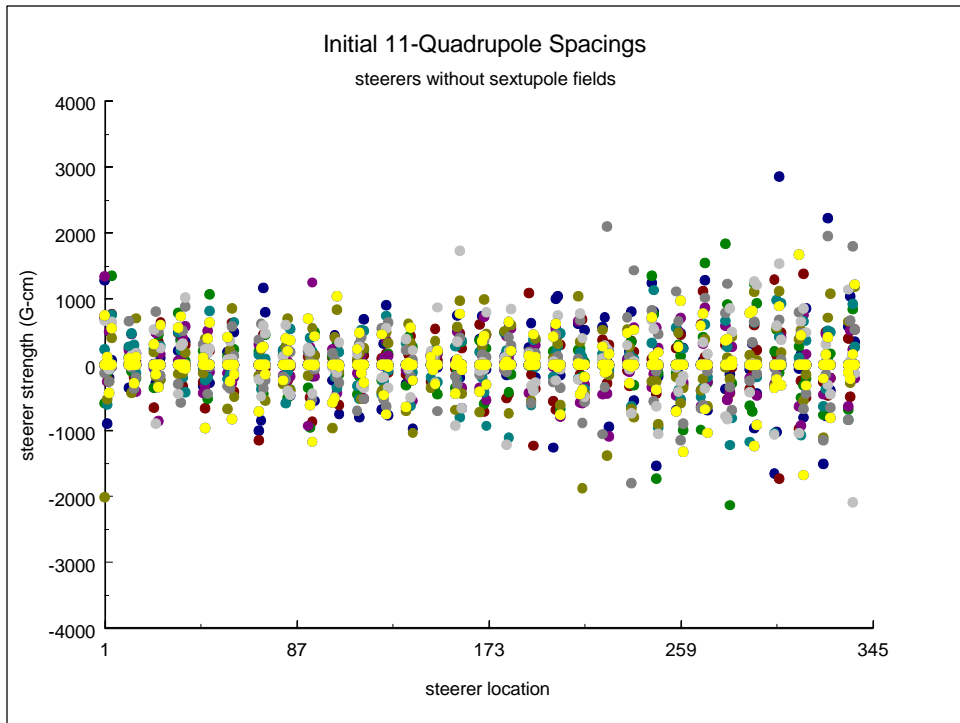


Figure 4. Steerer strengths for initial steering scheme with 11-quadrupole spacings without (top) and with (bottom) sextupole fields in steerers.

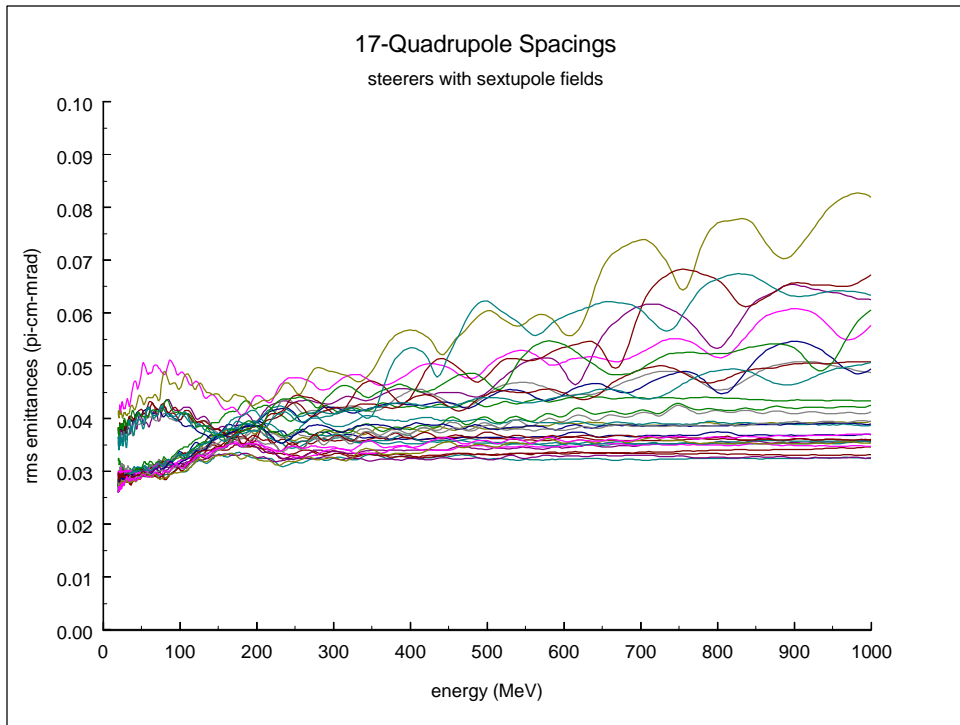
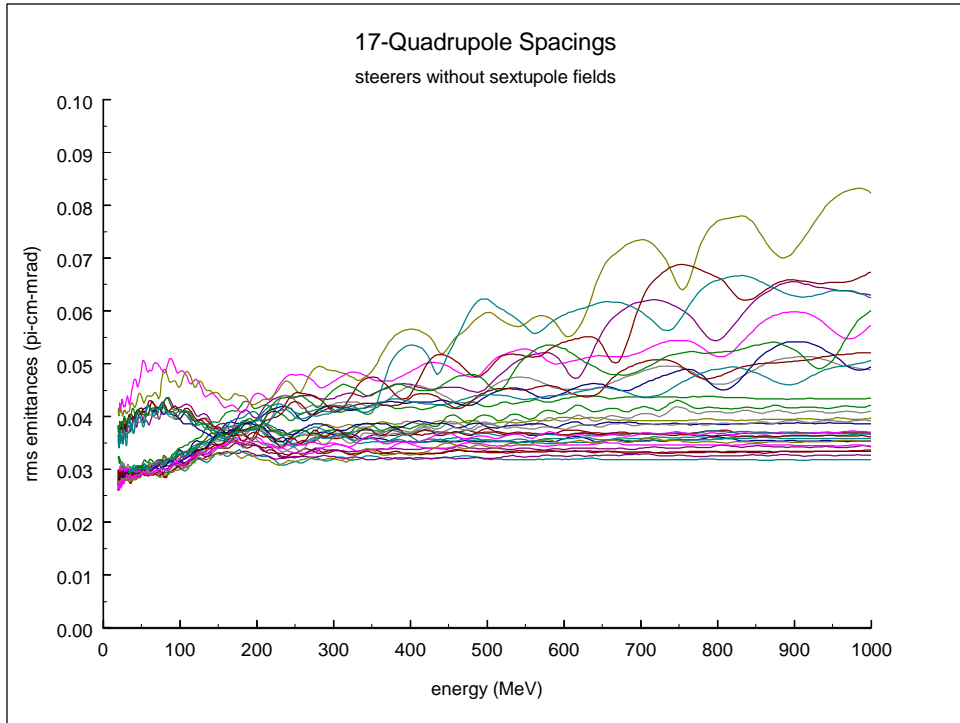


Figure 5. Transverse and longitudinal rms emittances for steering scheme with 17-quadrupole spacings without (top) and with (bottom) sextupole fields in steerers.

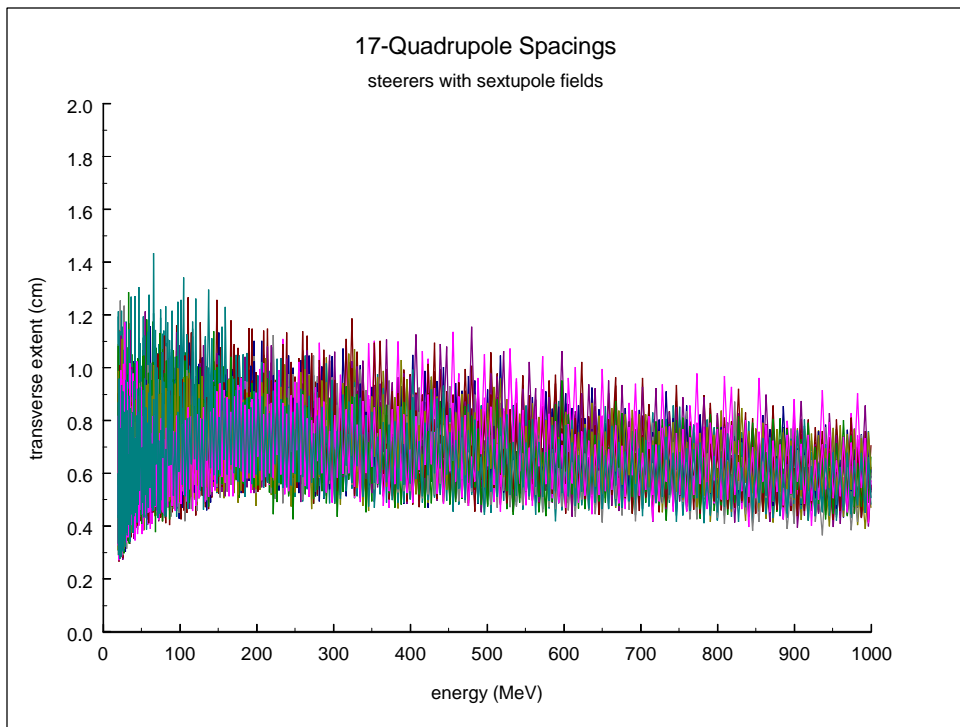
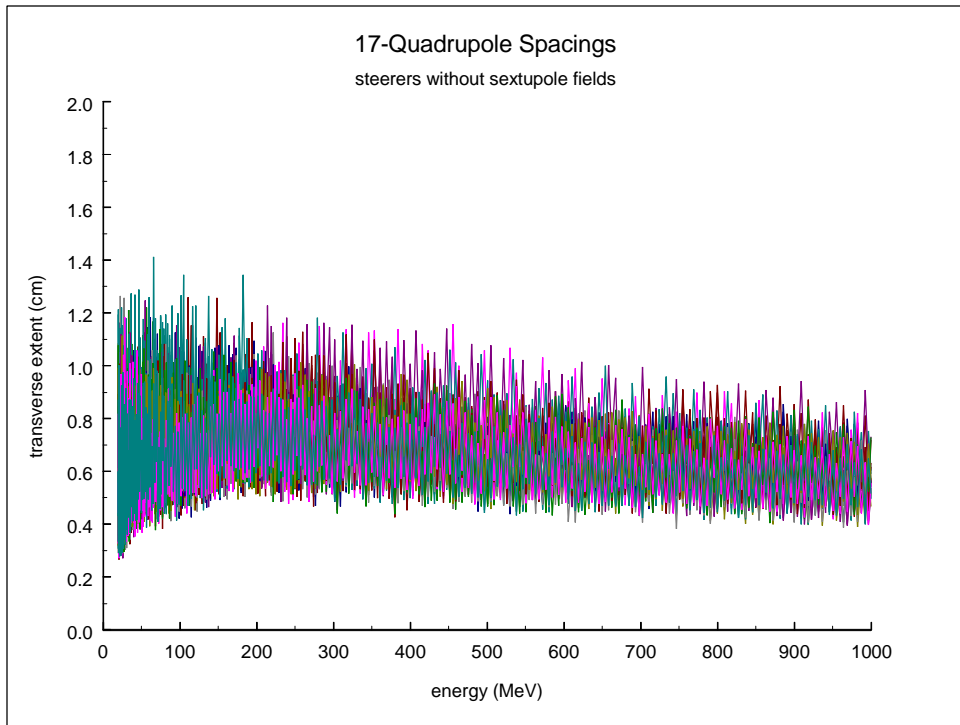


Figure 6. Maximum beam extents for steering scheme with 17-quadrupole spacings without (top) and with (bottom) sextupole fields in steerers.

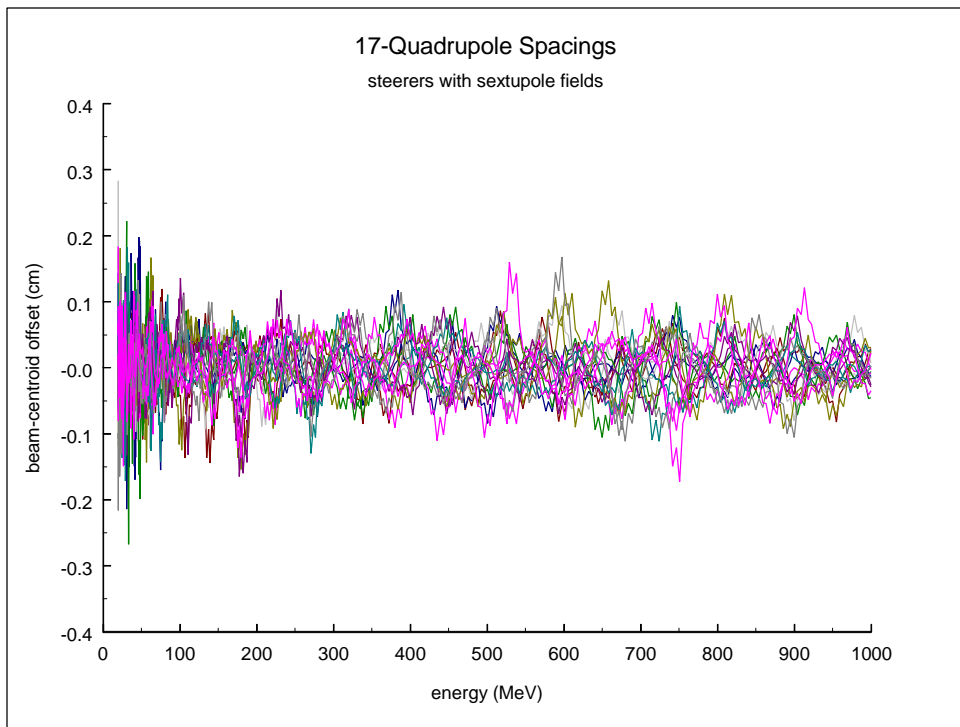
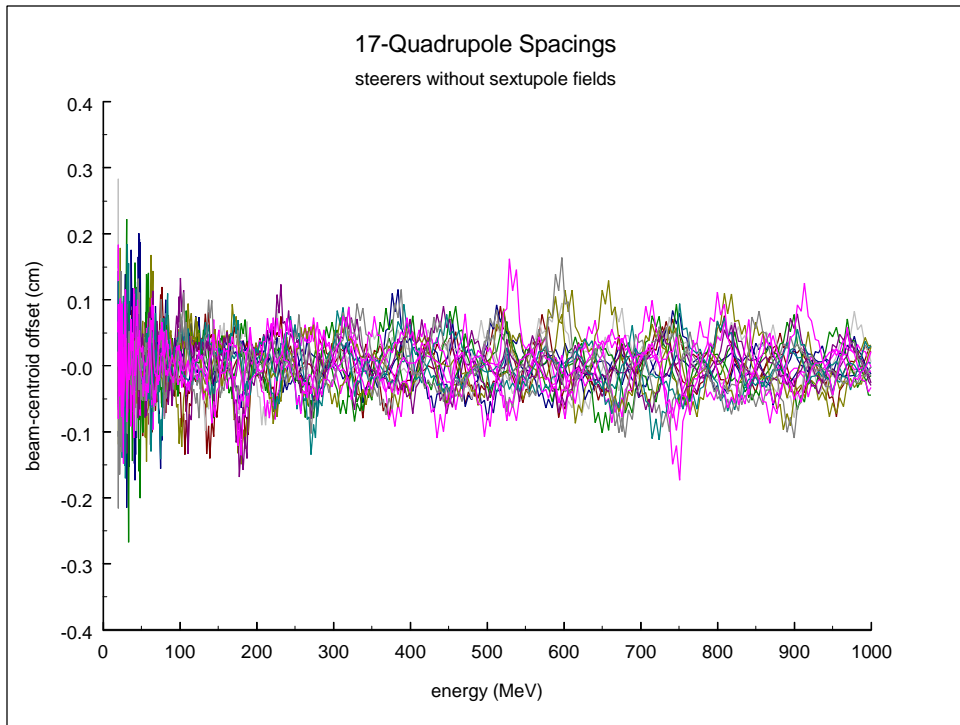


Figure 7. Beam-centroid excursions for steering scheme with 17-quadrupole spacings without (top) and with (bottom) sextupole fields in steerers.

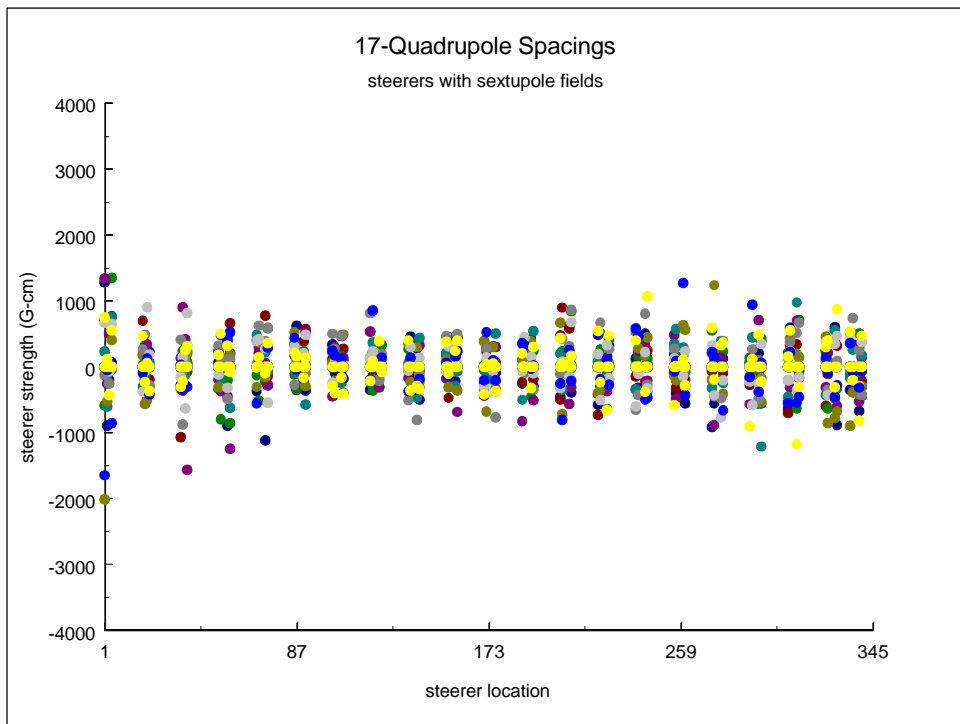
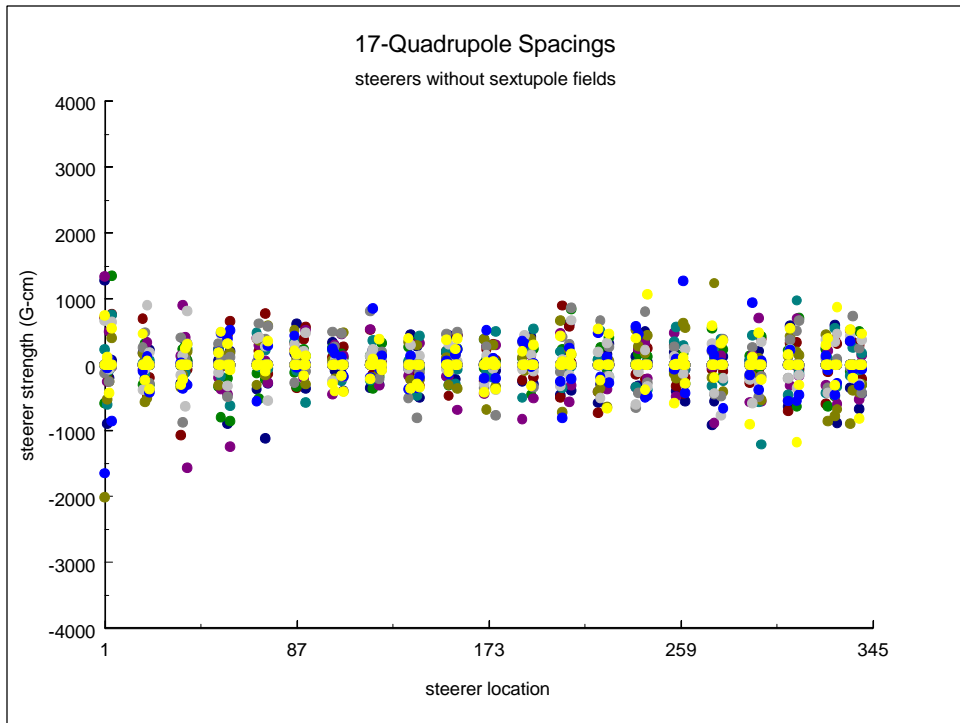


Figure 8. Steerer strengths for steering scheme with 17-quadrupole spacings without (top) and with (bottom) sextupole fields in steerers.

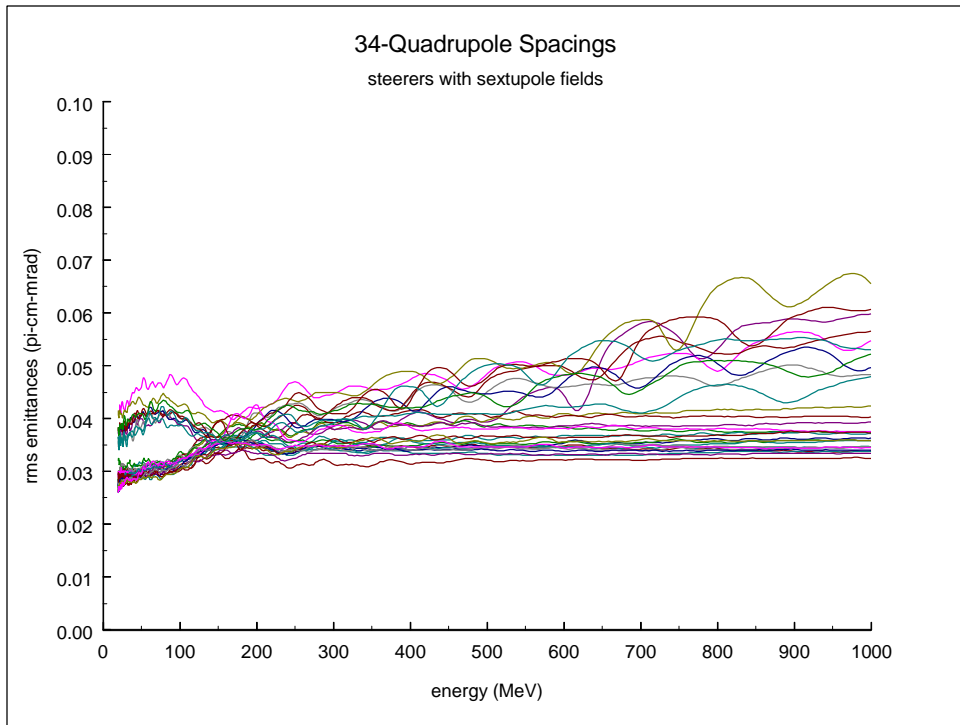
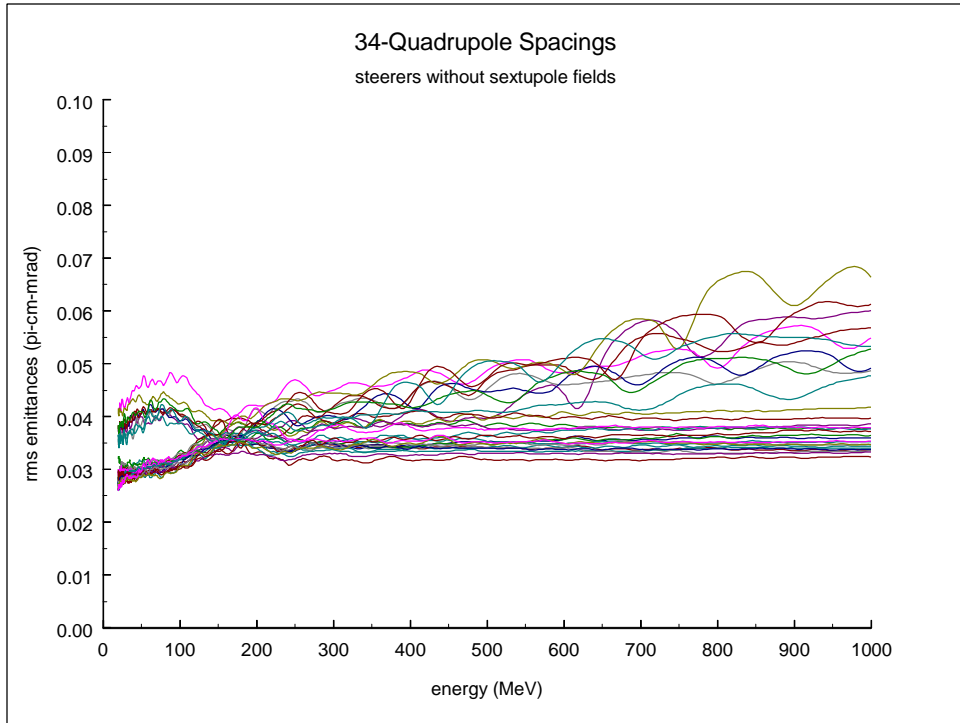


Figure 9. Transverse and longitudinal rms emittances for steering scheme with 34-quadrupole spacings without (top) and with (bottom) sextupole fields in steerers.

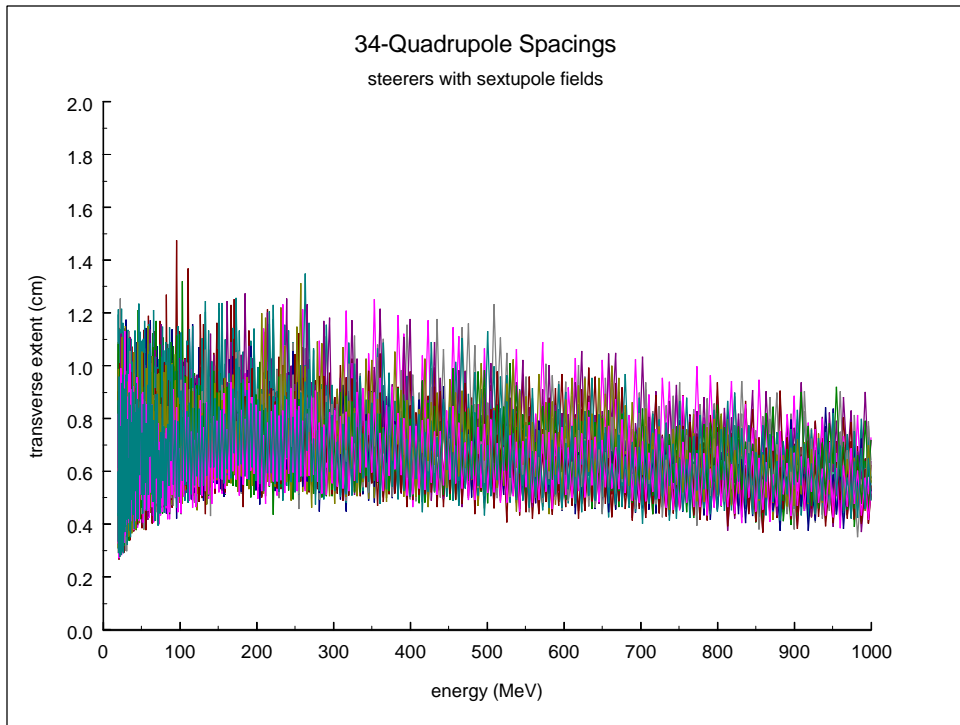
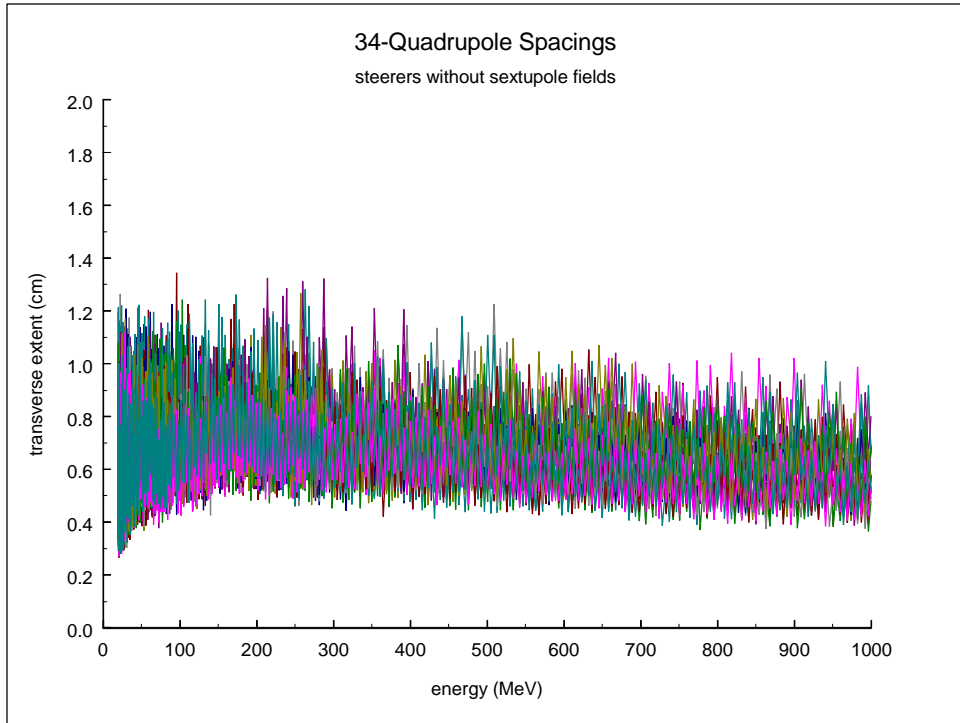


Figure 10. Beam extents for steering scheme with 34-quadrupole spacings without (top) and with (bottom) sextupole fields in steerers.

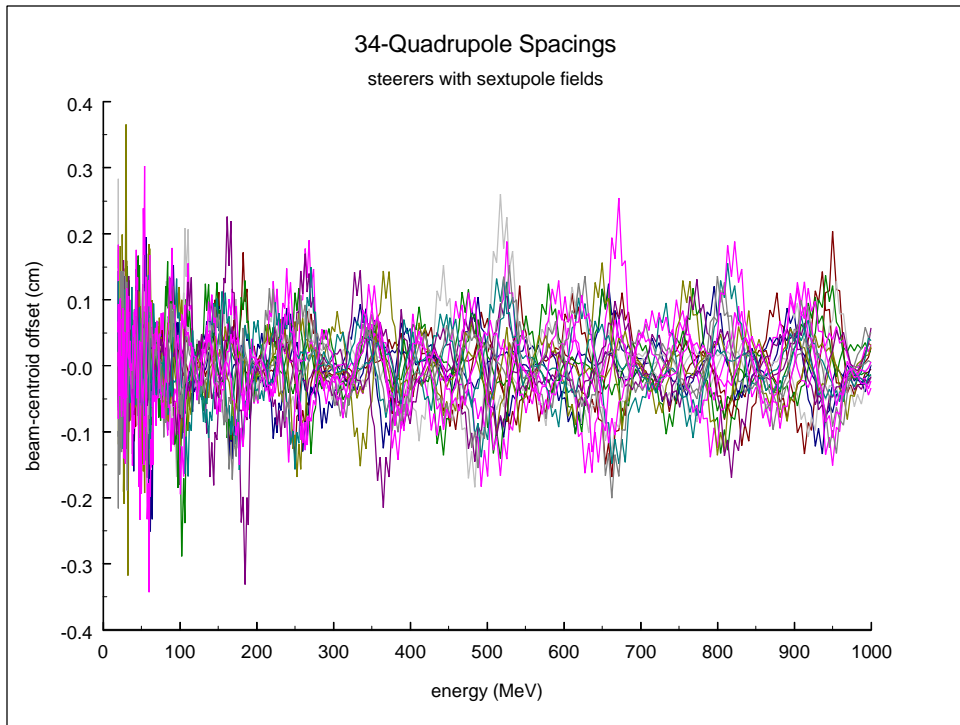
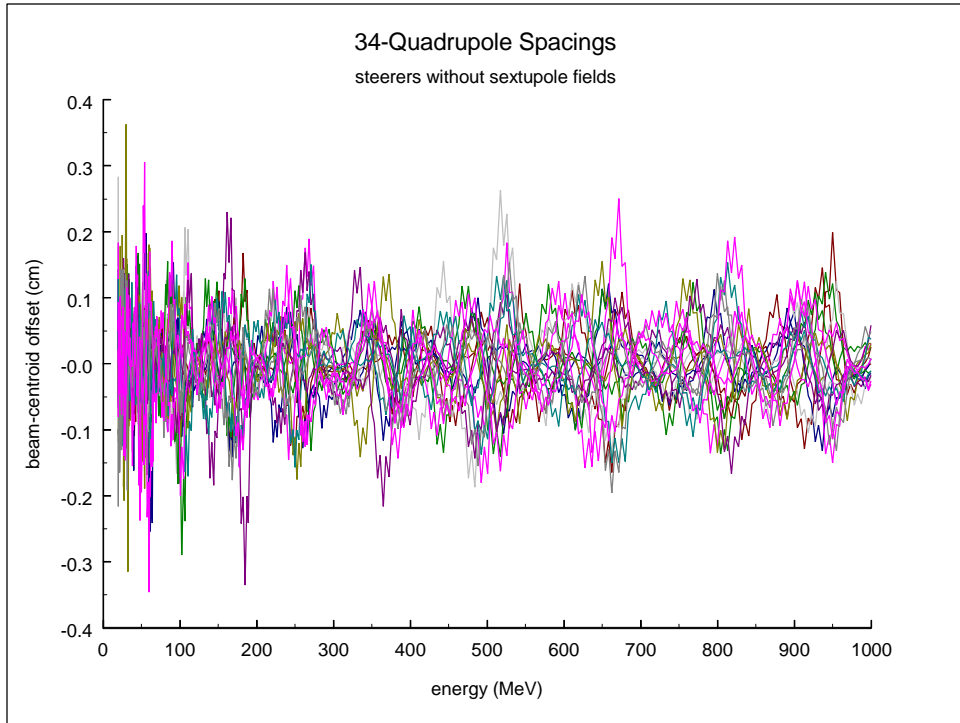


Figure 11. Beam-centroid excursions for steering scheme with 34-quadrupole spacings without (top) and with (bottom) sextupole fields in steerers.

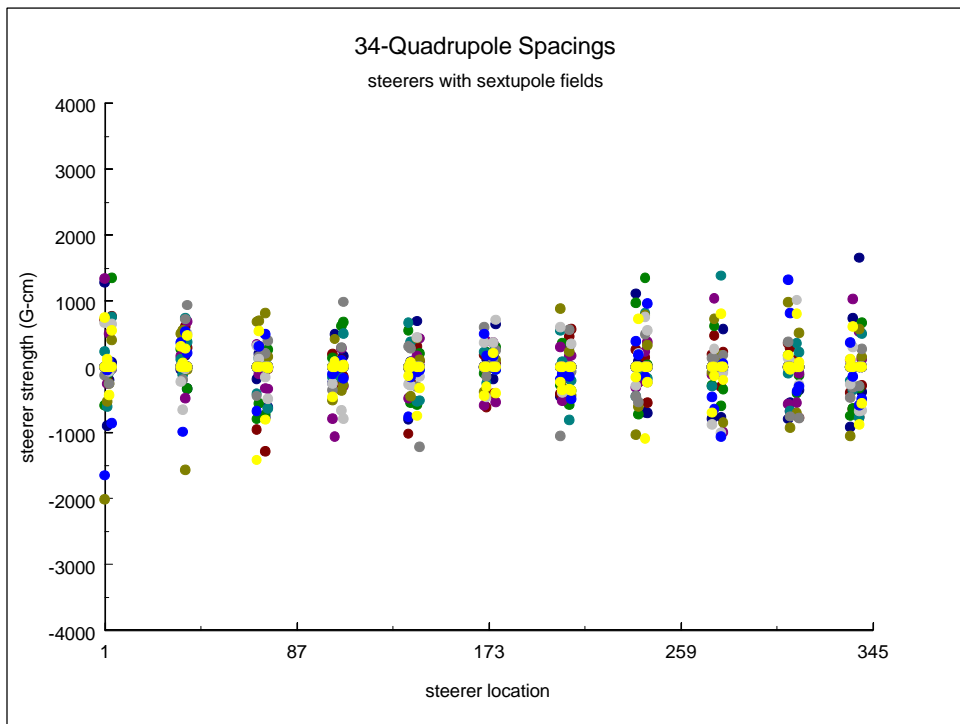
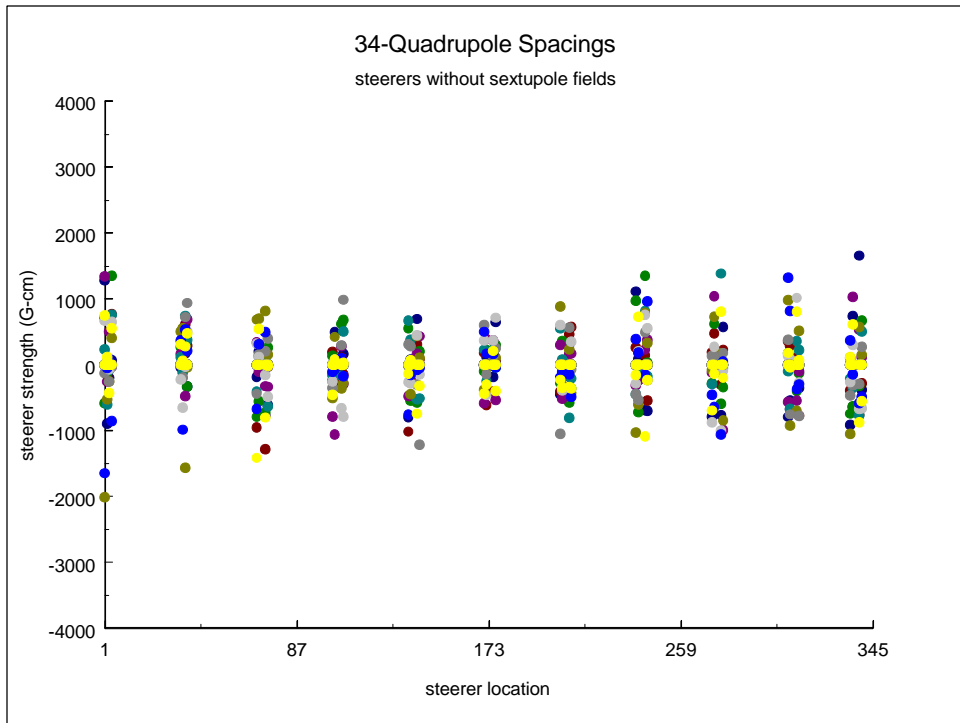


Figure 12. Steerer strengths for steering scheme with 34-quadrupole spacings without (top) and with (bottom) sextupole fields in steerers.

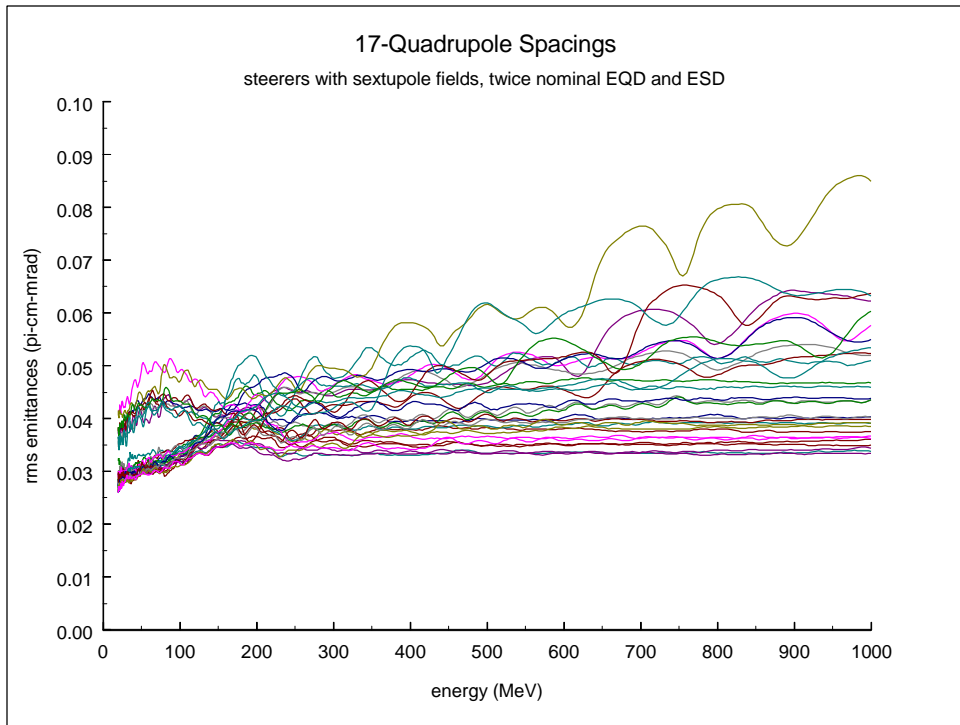
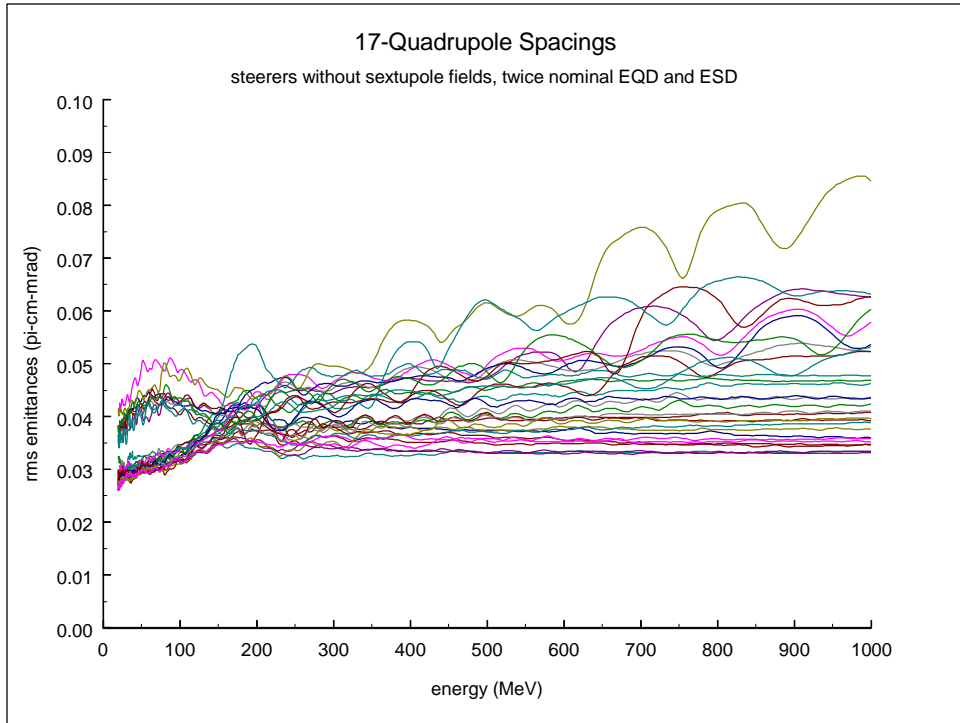


Figure 13. Rms emittances for steering scheme with 17-quadrupole spacings w/o (top) and with (bottom) sextupole fields in steerers, at twice nominal EQD and ESD.

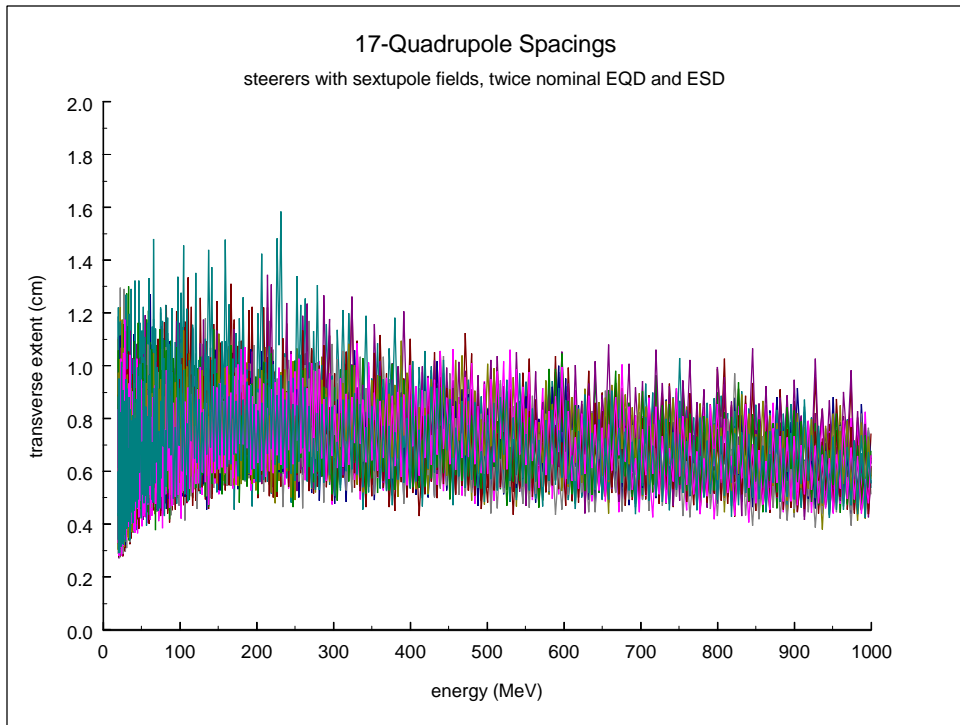
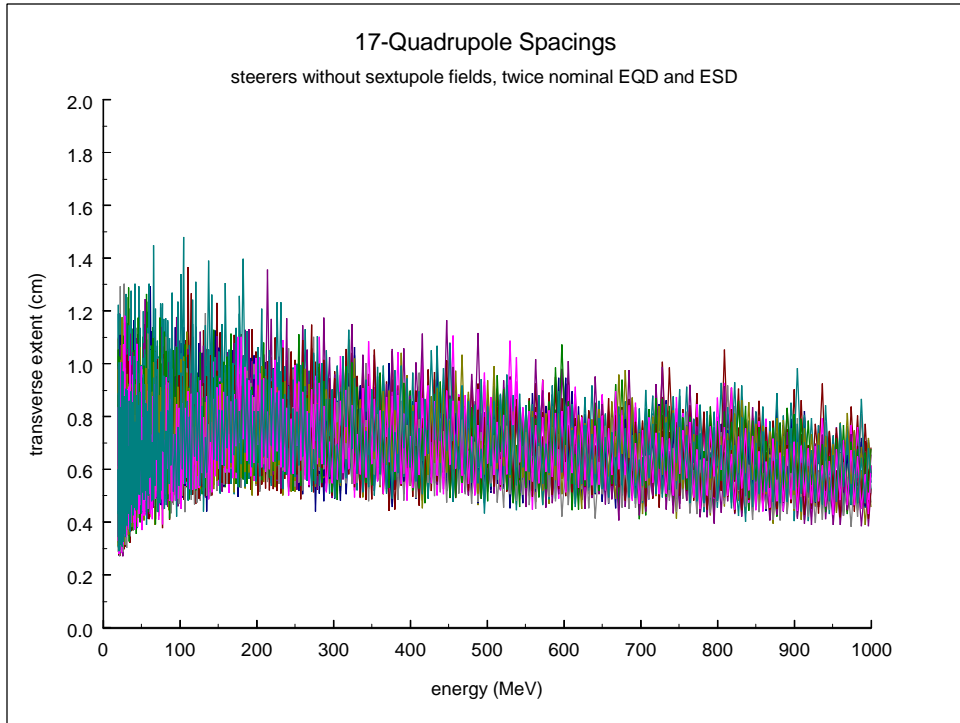


Figure 14. Maximum beam extents for steering scheme with 17-quadrupole spacings w/o (top) and with (bottom) sextupole fields in steerers at twice nominal EQD and ESD.

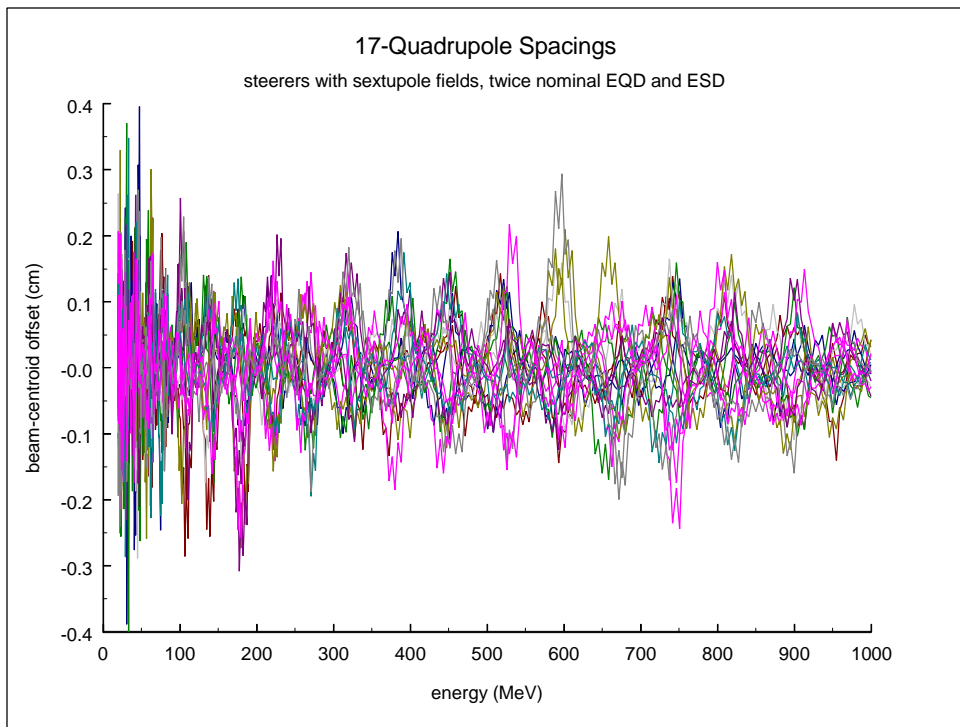
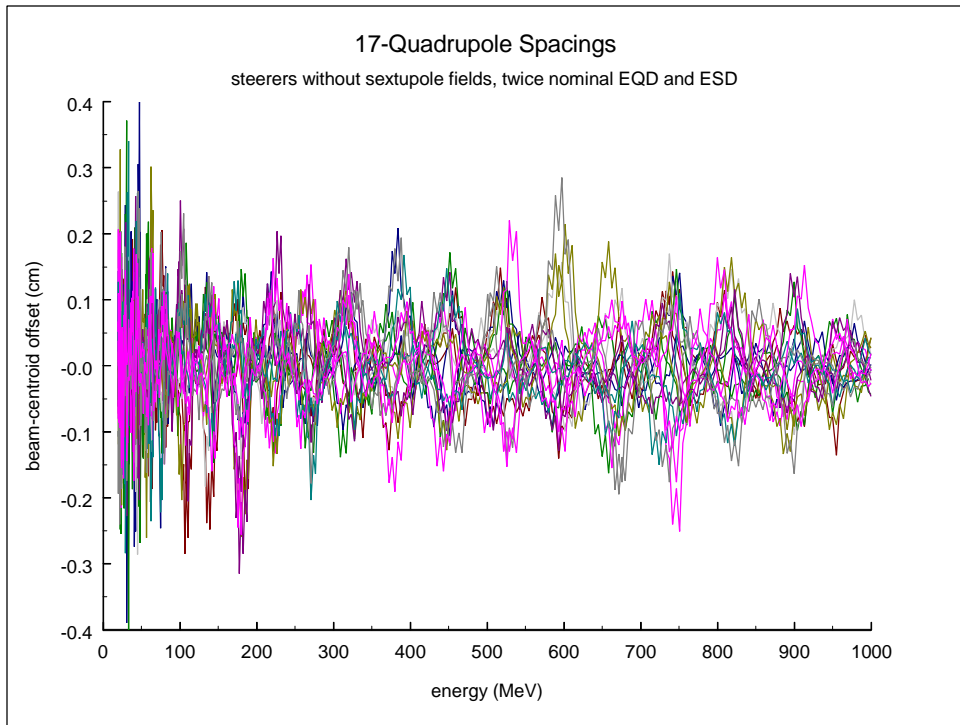


Figure 15. Beam-centroid excursions for steering scheme with 17-quadrupole spacings w/o (top) and with (bottom) sextupole fields in steerers, at twice nominal EQD and ESD.

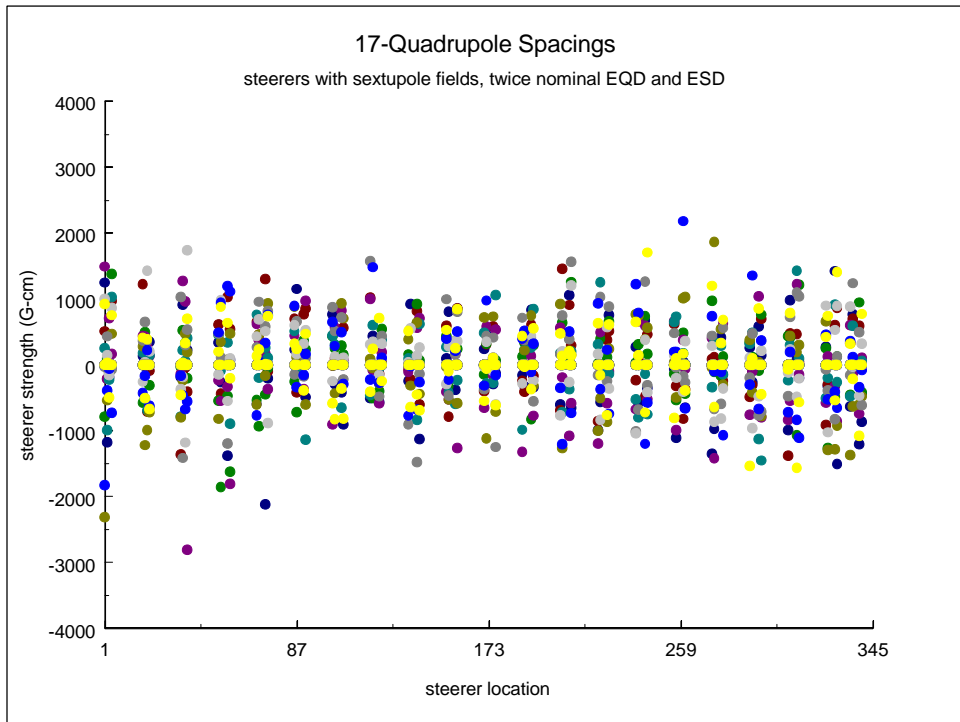
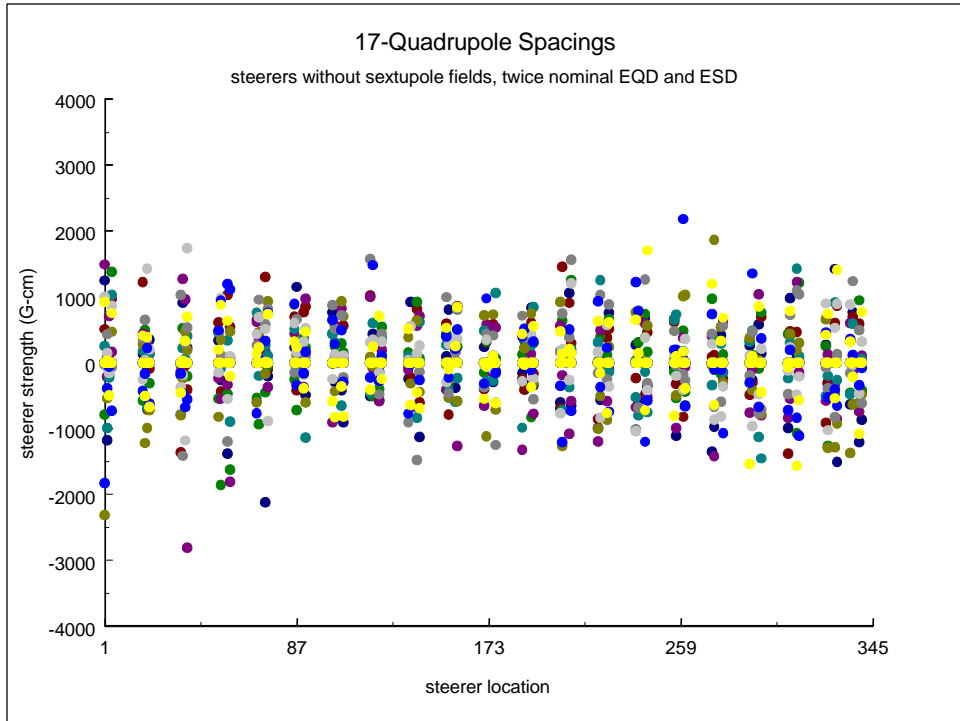


Figure 16. Steerer strengths for steering scheme with 17-quadrupole spacings w/o (top) and with (bottom) sextupole fields in steerers, at twice nominal EQD and ESD.

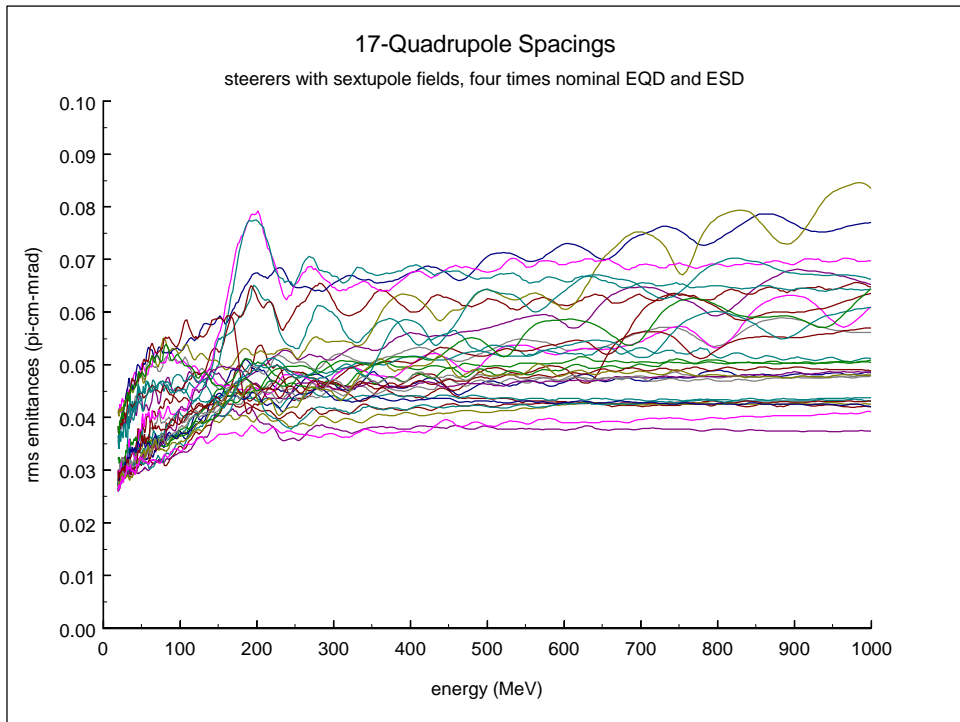
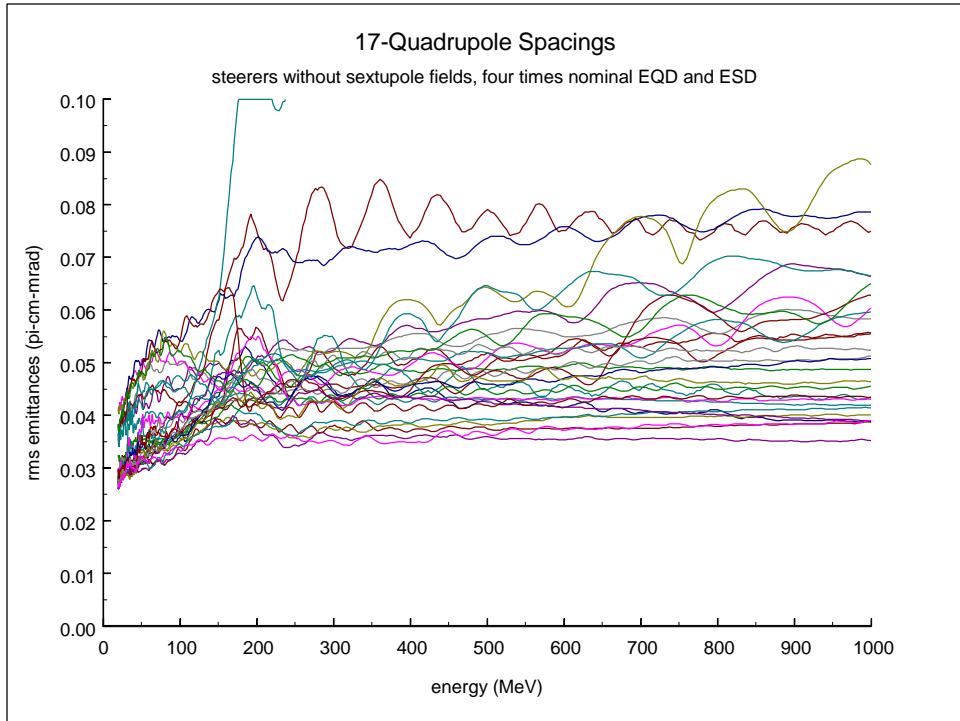


Figure 17. Rms emittances for steering scheme with 17-quadrupole spacings w/o (top) and with (bottom) sextupole fields in steerers, at four times nominal EQD and ESD.

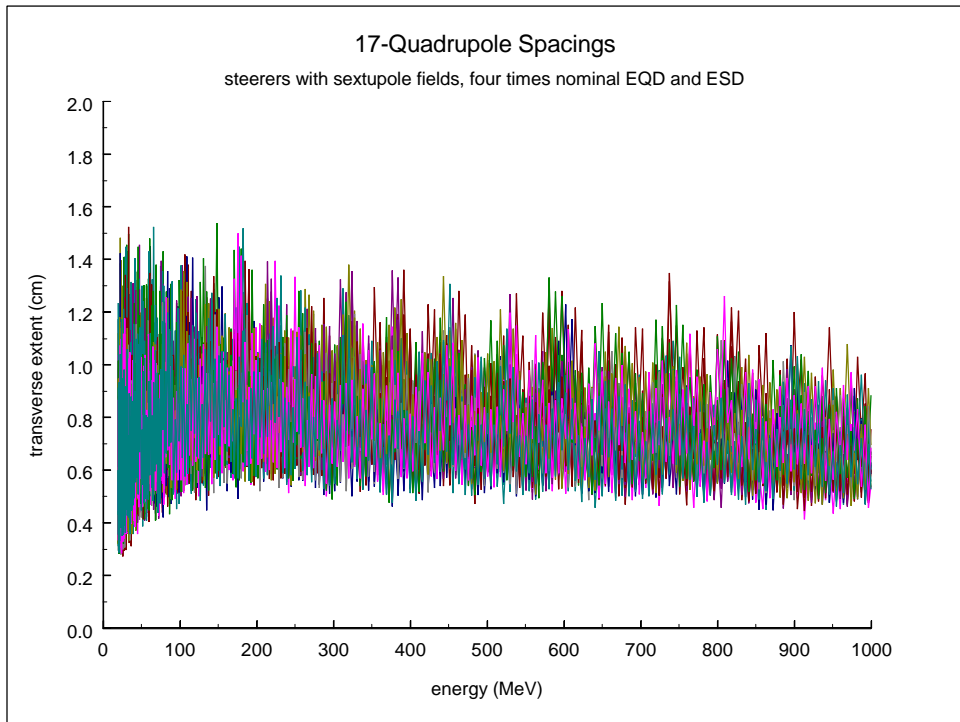
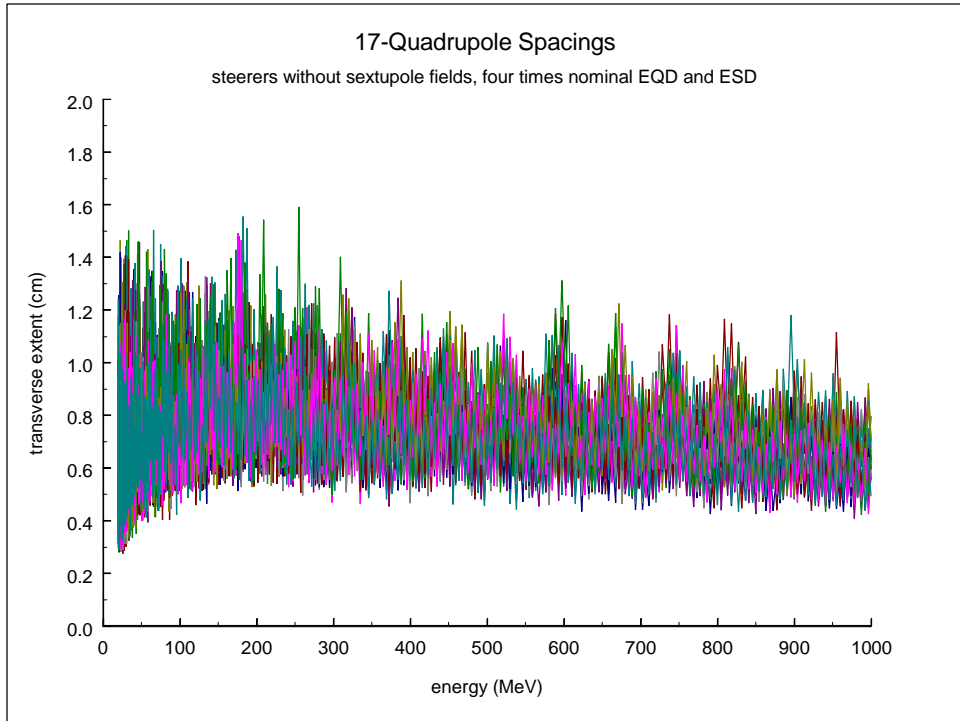


Figure 18. Maximum beam extents for steering scheme with 17-quadrupole spacings w/o (top) and with (bottom) sextupole fields in steerers, at four times nominal EQD and ESD.

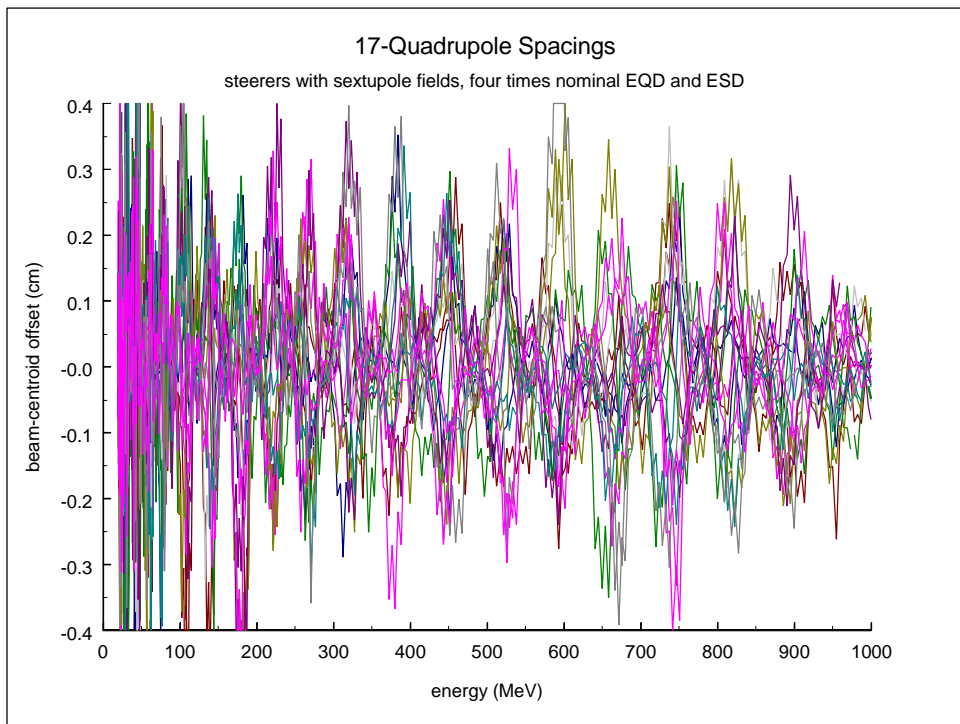
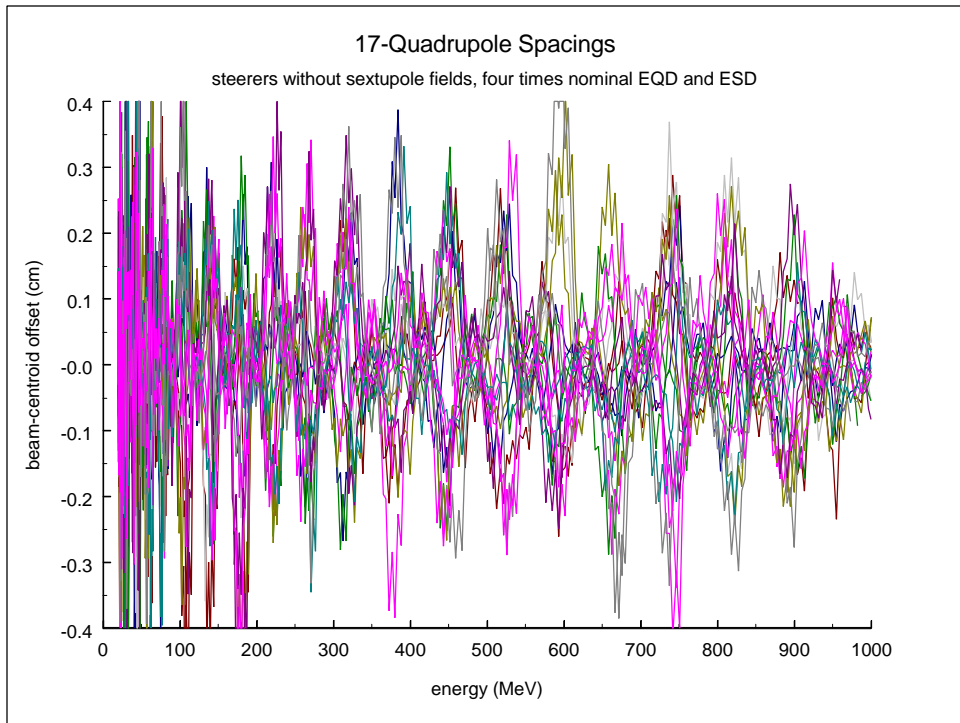


Figure 19. Beam centroids for steering scheme with 17-quadrupole spacings w/o (top) and with (bottom) sextupole fields in steerers, at four times nominal EQD and ESD.

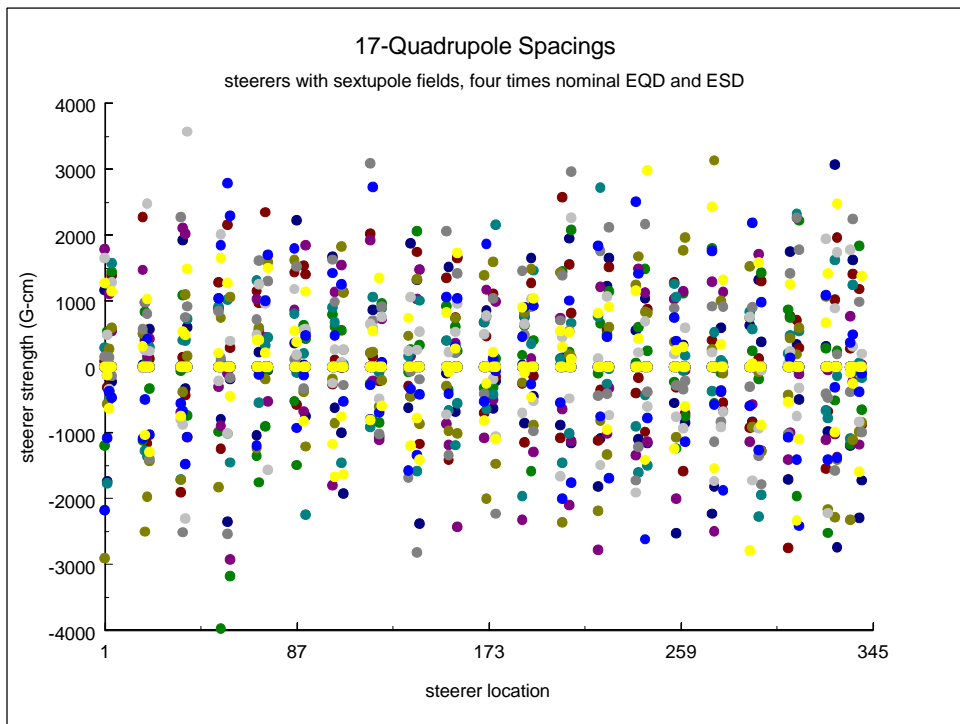
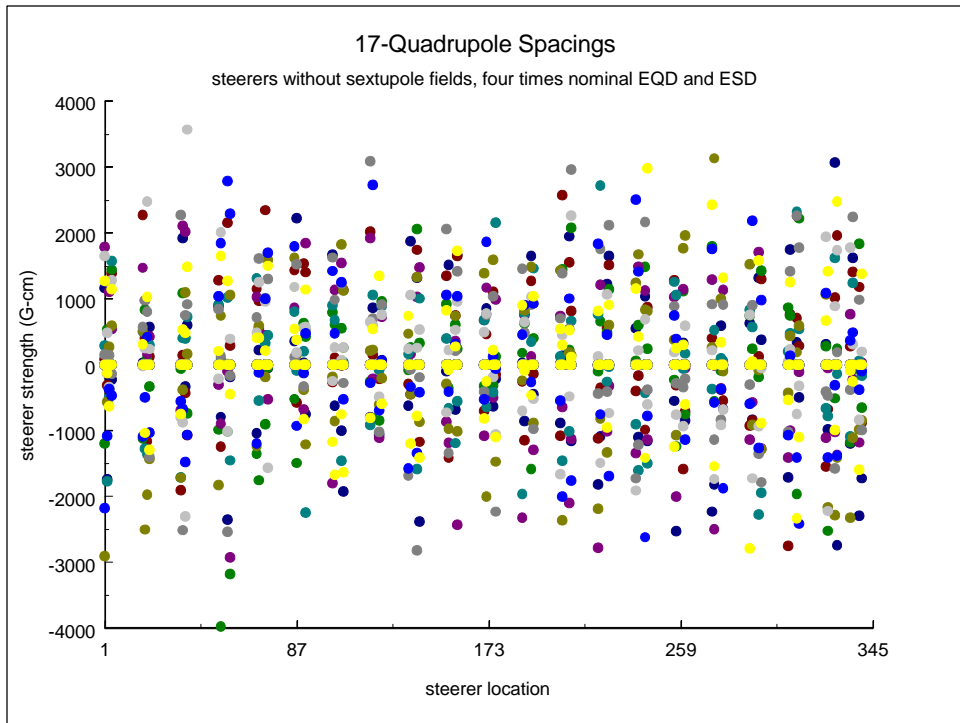


Figure 20. Steerer strengths for steering scheme with 17-quadrupole spacings w/o (top) and with (bottom) sextupole fields in steerers, at four times nominal EQD and ESD.

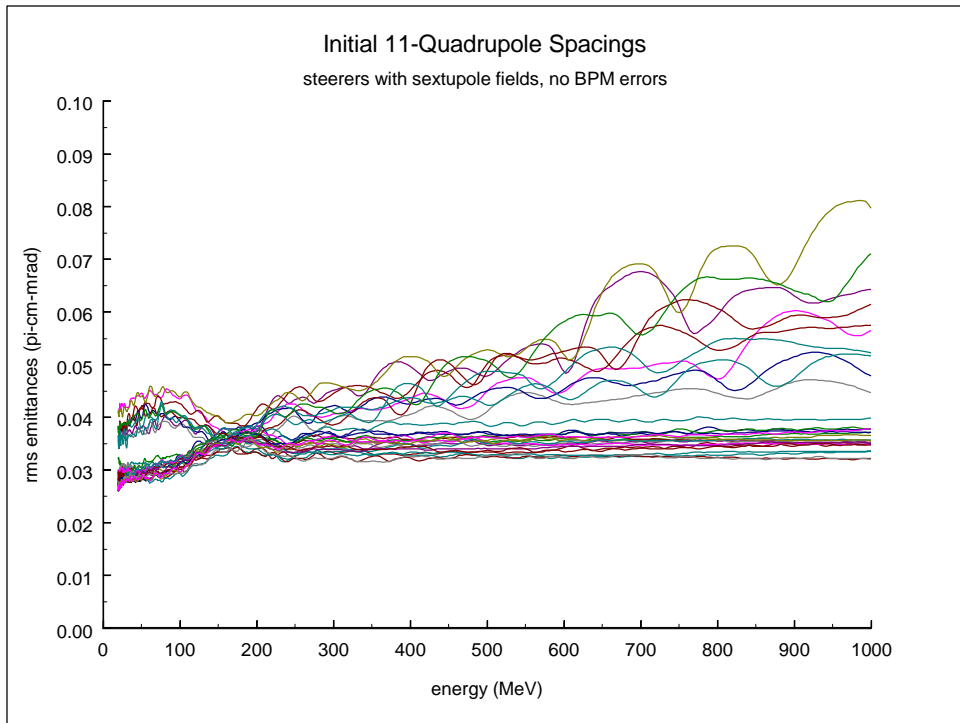


Figure 21. Steering scheme with initial 11-quadrupole spacings, no BPM errors.

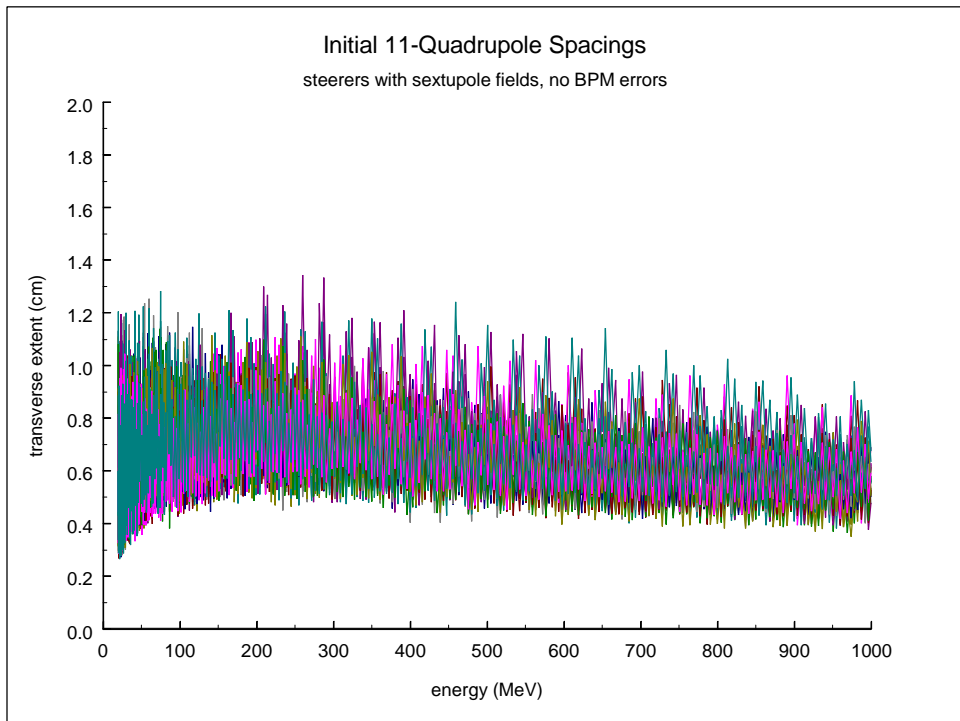


Figure 22. Steering scheme with initial 11-quadrupole spacings, no BPM errors.

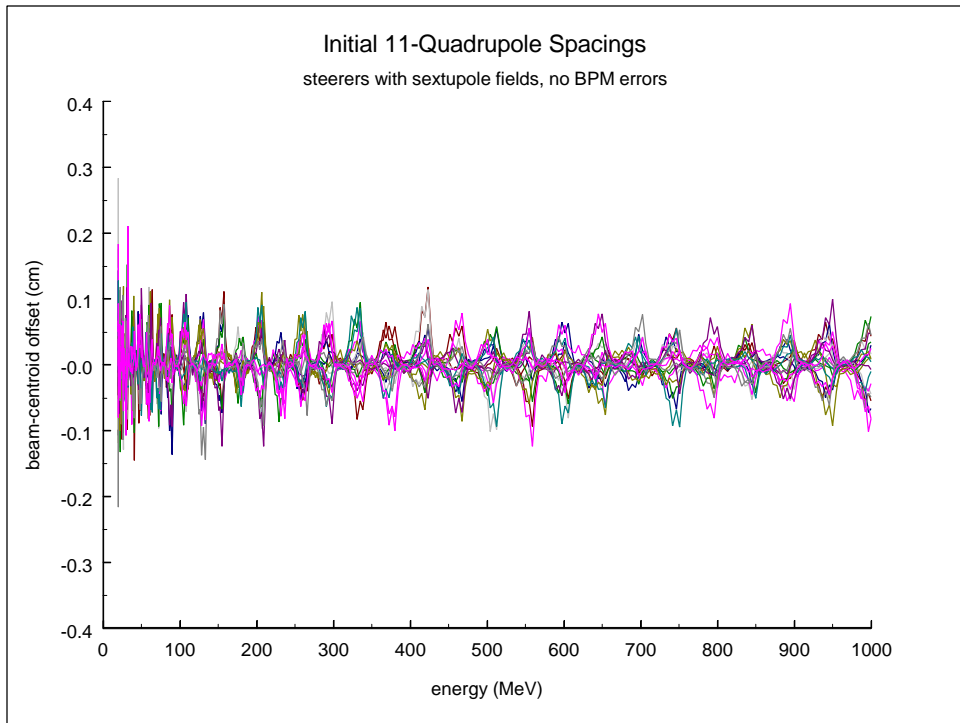


Figure 23. Steering scheme with initial 11-quadrupole spacings, no BPM errors.

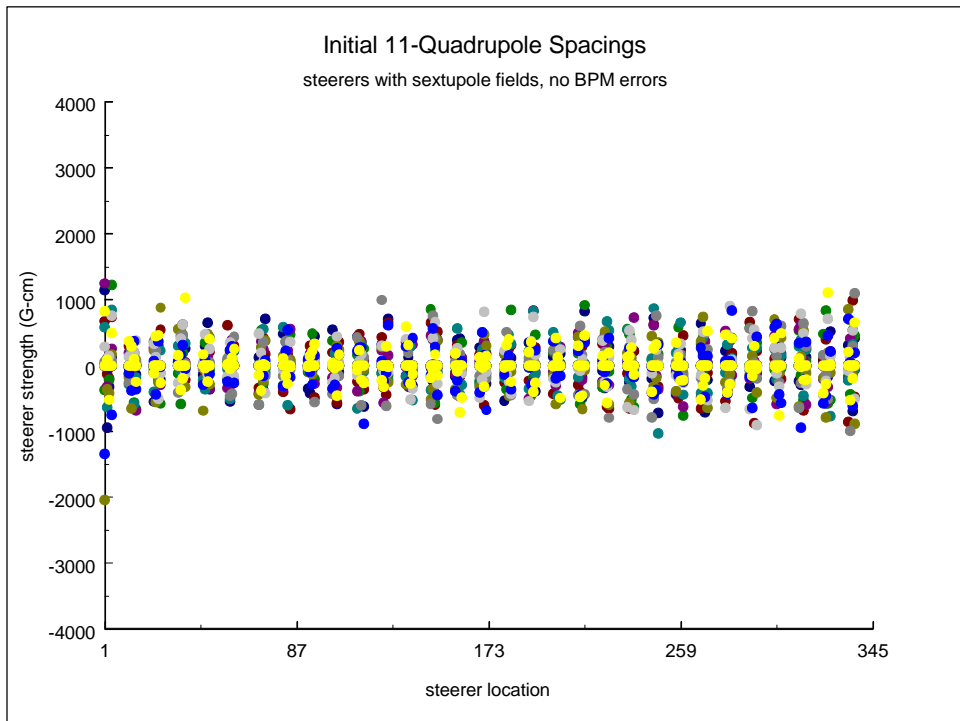


Figure 24. Steering scheme with initial 11-quadrupole spacings, no BPM errors.

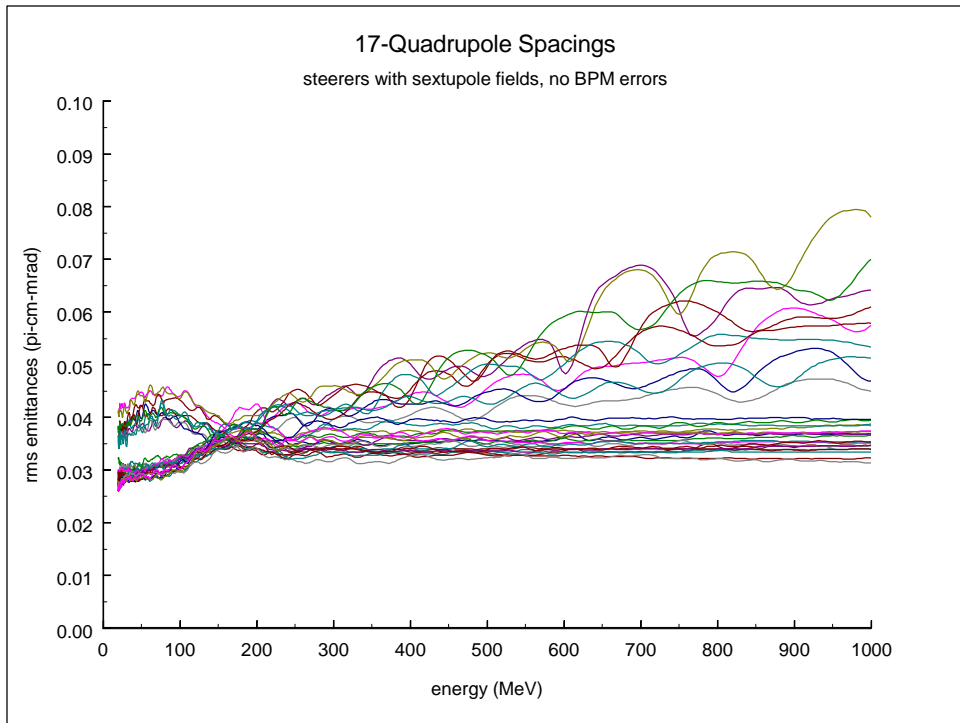


Figure 25. Steering scheme with 17-quadrupole spacings, no BPM errors.

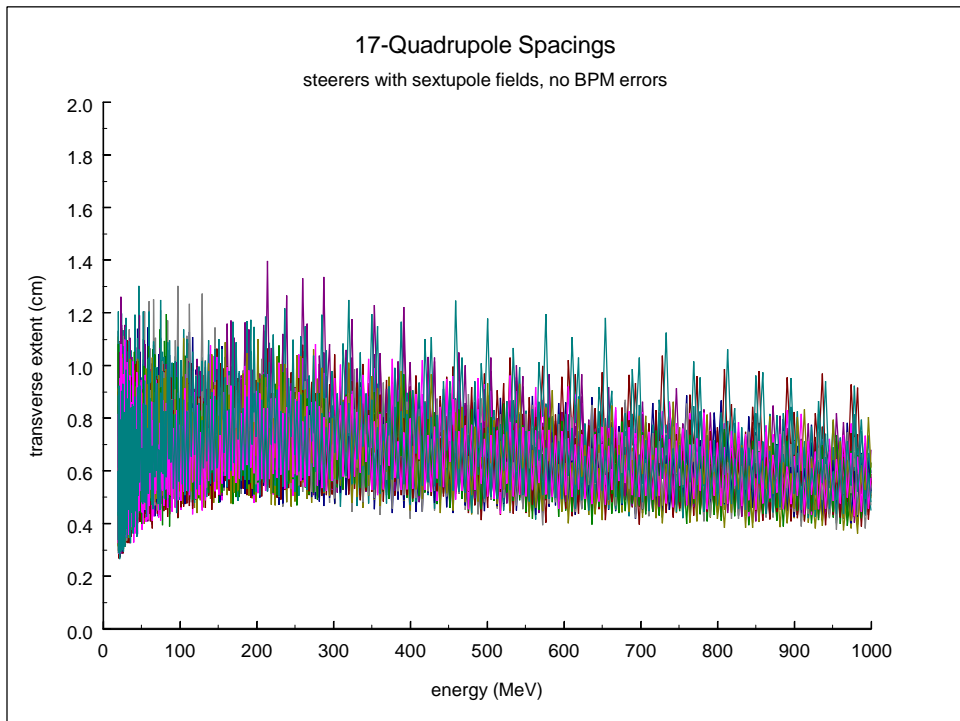


Figure 26. Steering scheme with 17-quadrupole spacings, no BPM errors.

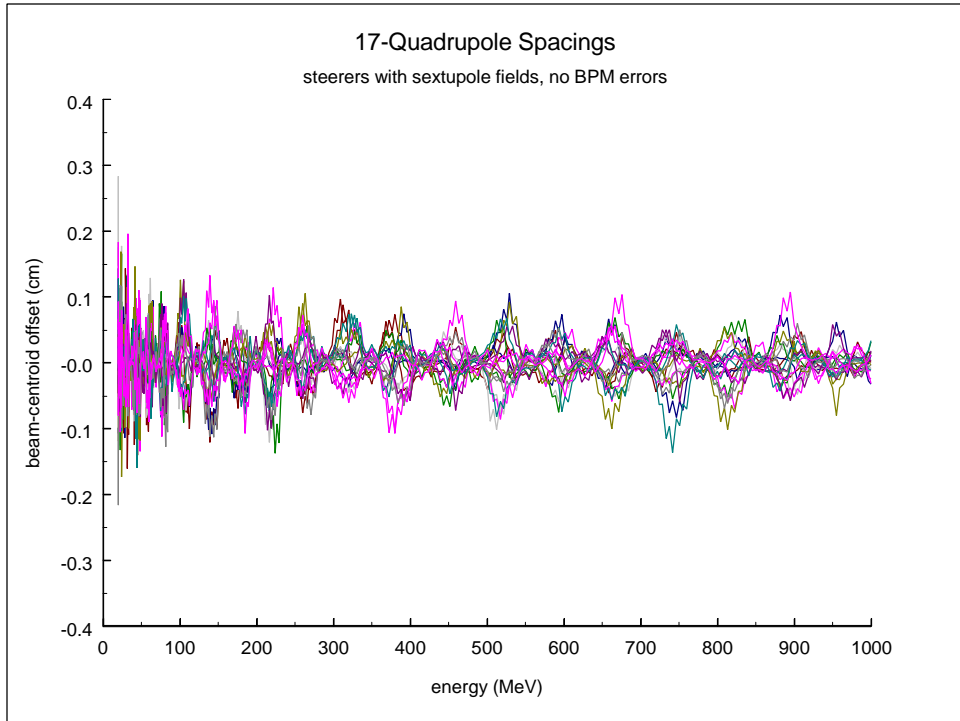


Figure 27. Steering scheme with 17-quadrupole spacings, no BPM errors.

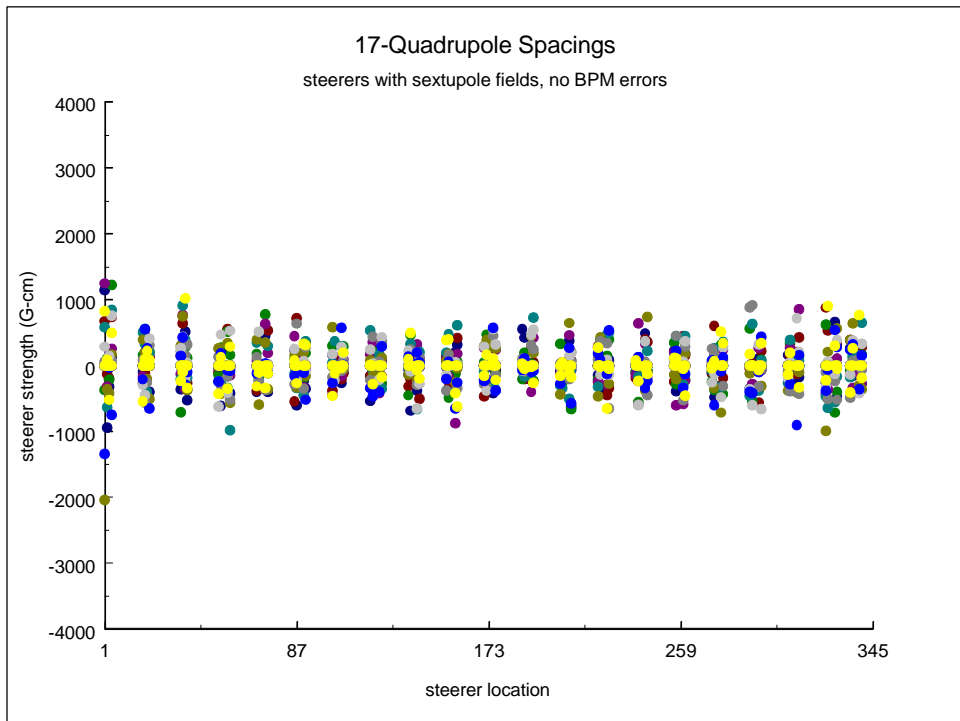


Figure 28. Steering scheme with 17-quadrupole spacings, no BPM errors.

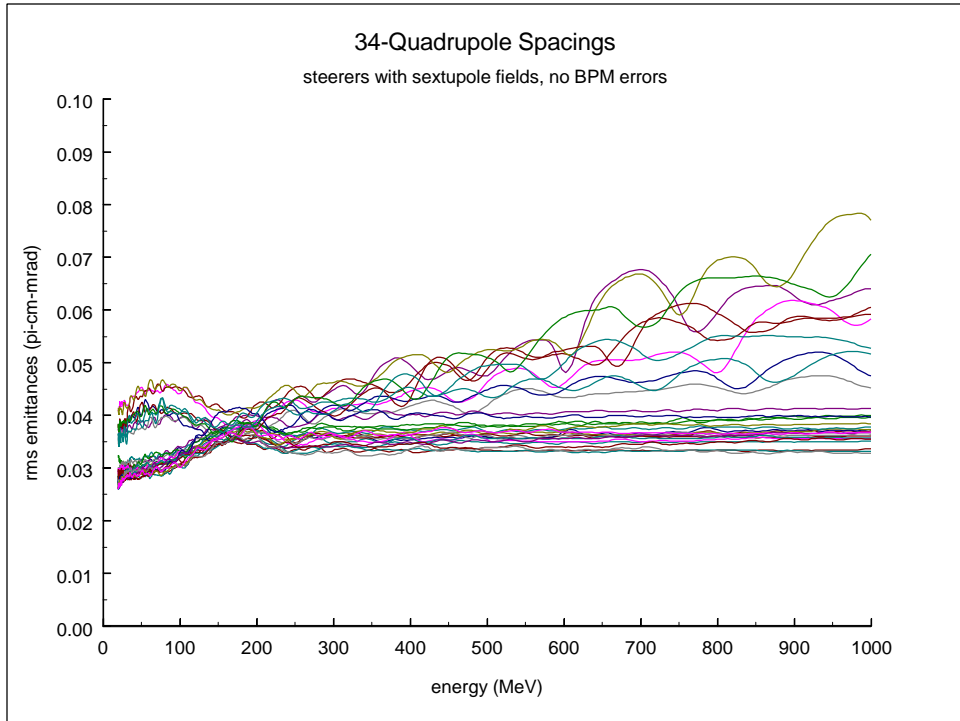


Figure 29. Steering scheme with 34-quadrupole spacings, no BPM errors.

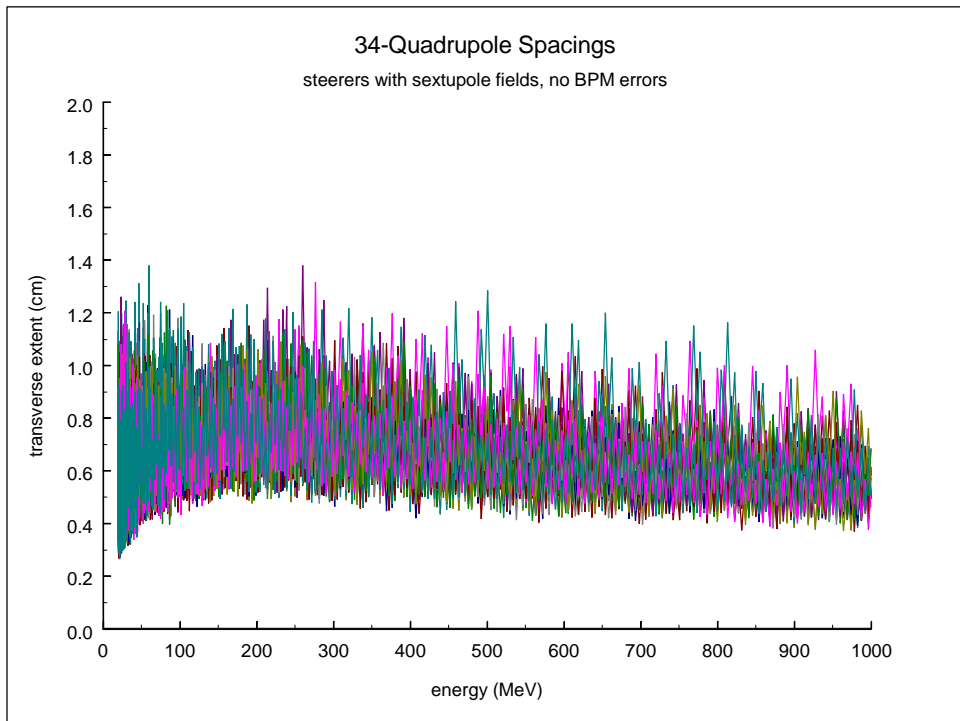


Figure 30. Steering scheme with 34-quadrupole spacings, no BPM errors.

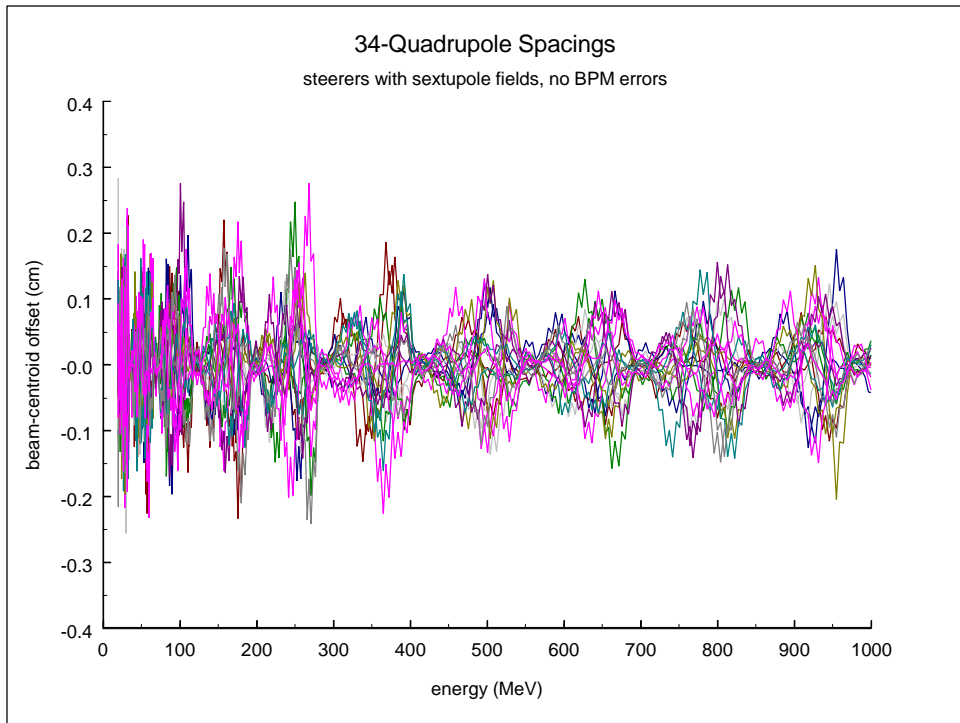


Figure 31. Steering scheme with 34-quadrupole spacings, no BPM errors.

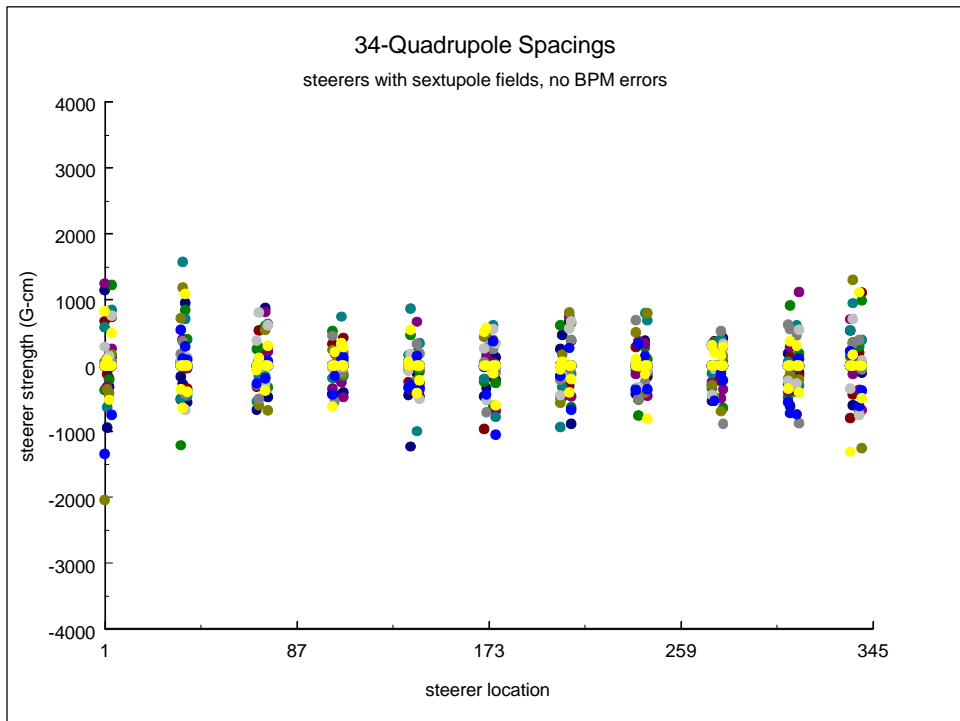


Figure 32. Steering scheme with 34-quadrupole spacings, no BPM errors.

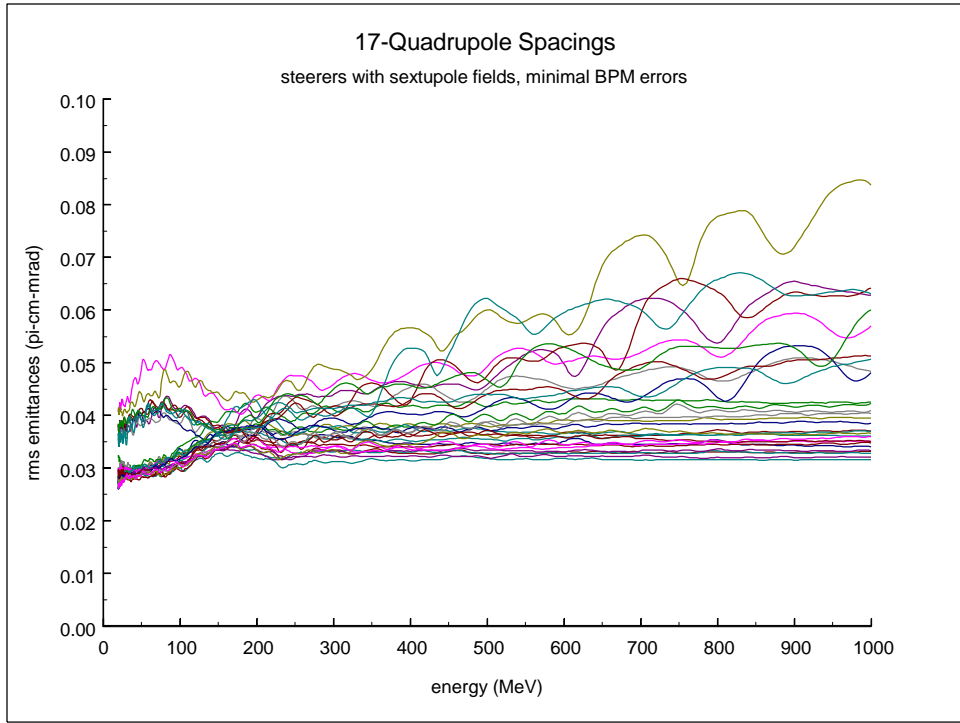


Figure 33. Steering scheme with 17-quadrupole spacings, minimal BPM errors.

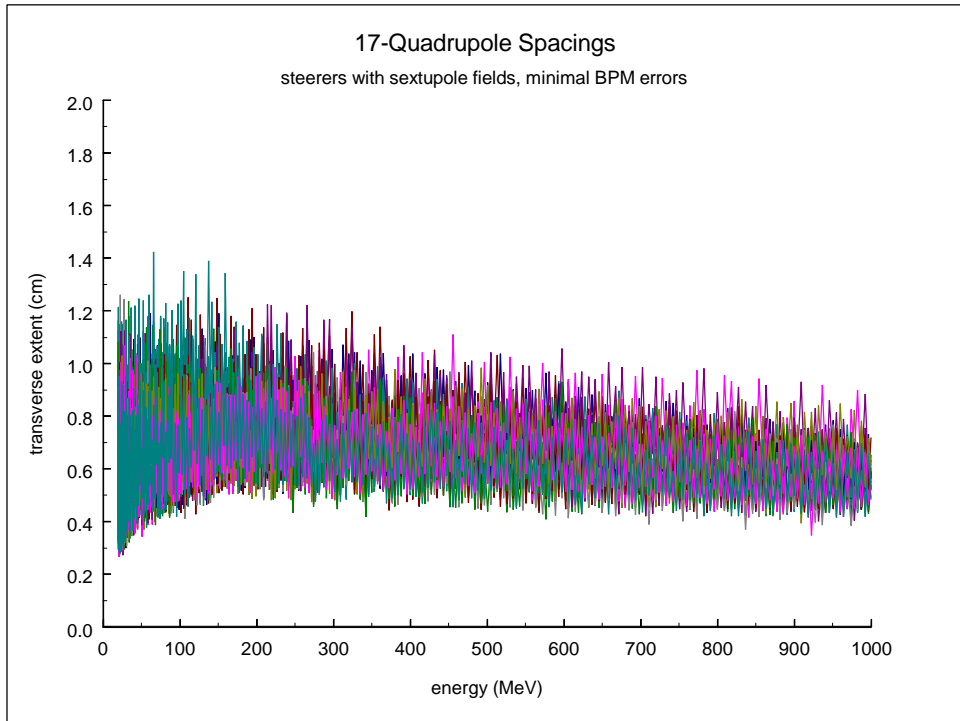


Figure 34. Steering scheme with 17-quadrupole spacings, minimal BPM errors.

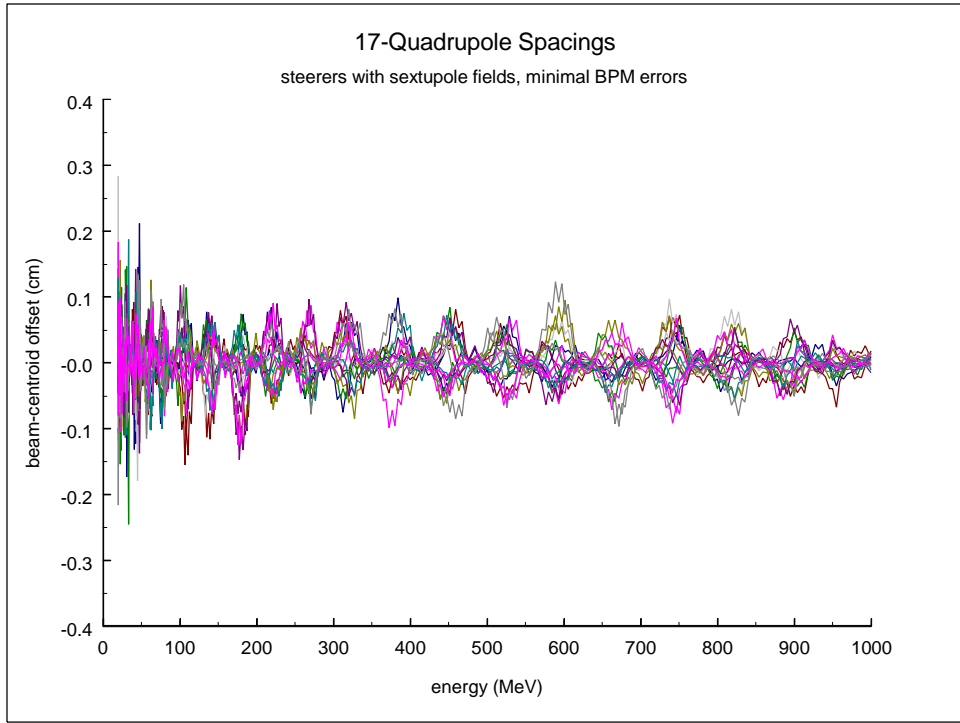


Figure 35. Steering scheme with 17-quadropole spacings, minimal BPM errors.

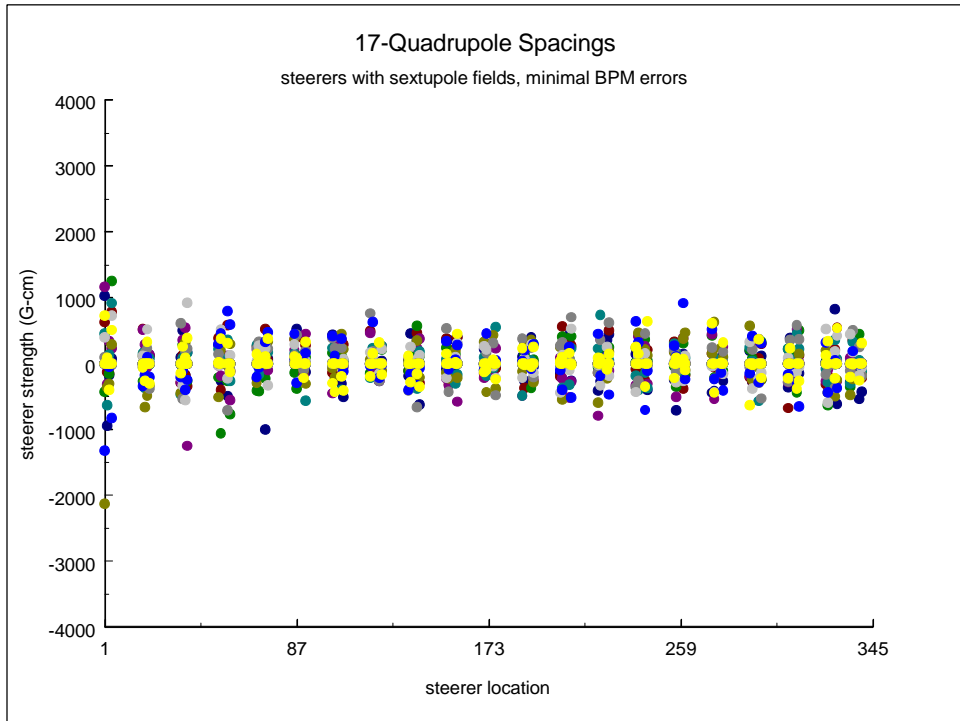


Figure 36. Steering scheme with 17-quadropole spacings, minimal BPM errors.

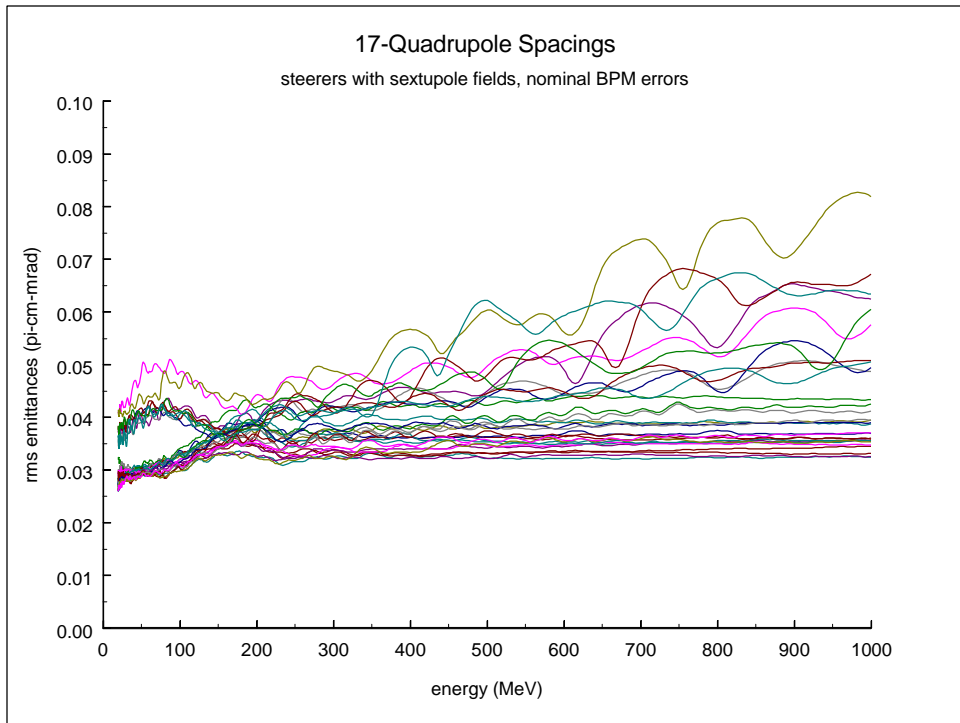


Figure 37. Steering scheme with 17-quadrupole spacings, nominal BPM errors.

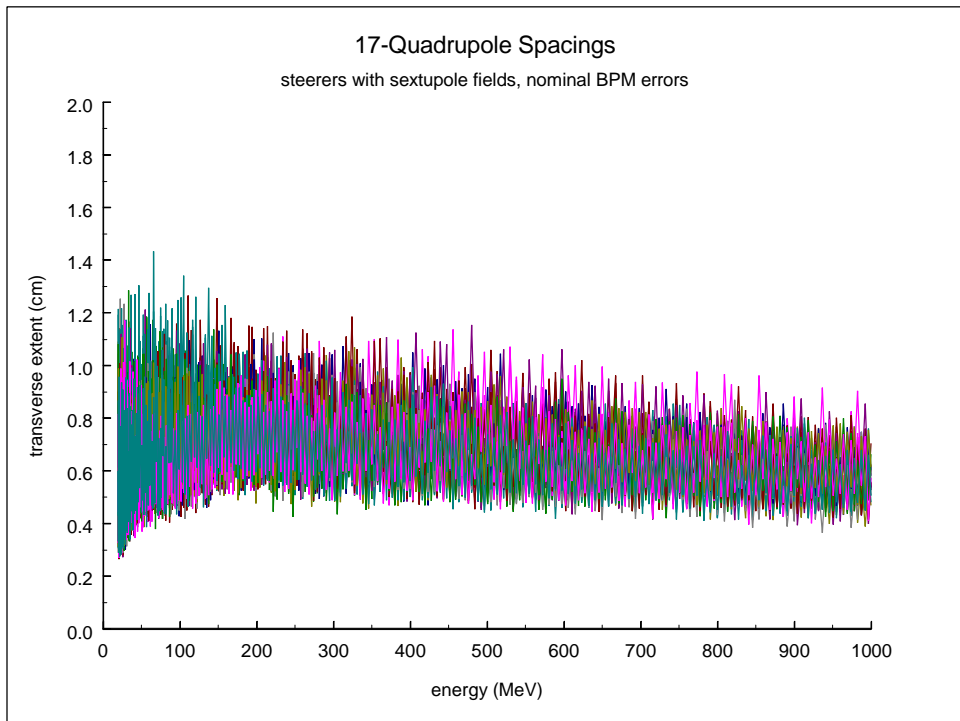


Figure 38. Steering scheme with 17-quadrupole spacings, nominal BPM errors.

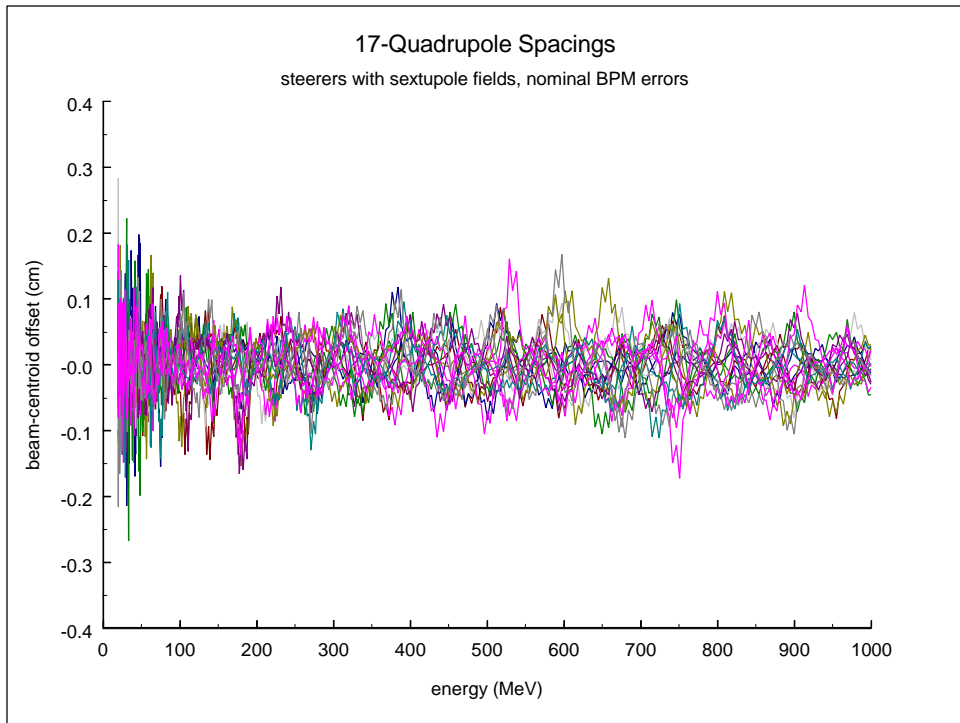


Figure 39. Steering scheme with 17-quadrupole spacings, nominal BPM errors.

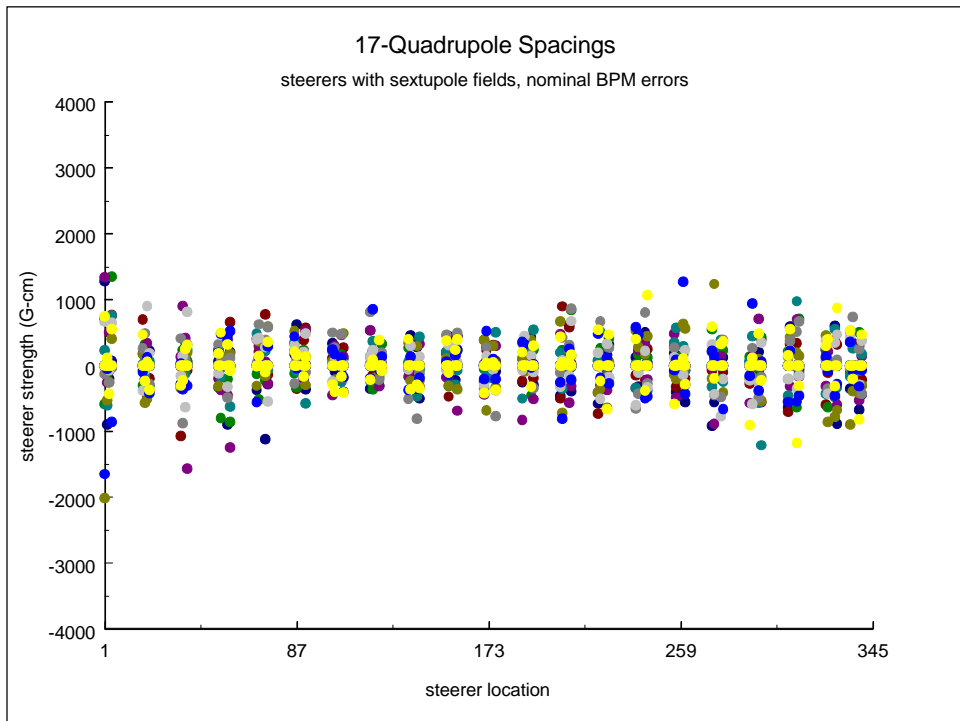


Figure 40. Steering scheme with 17-quadrupole spacings, nominal BPM errors.

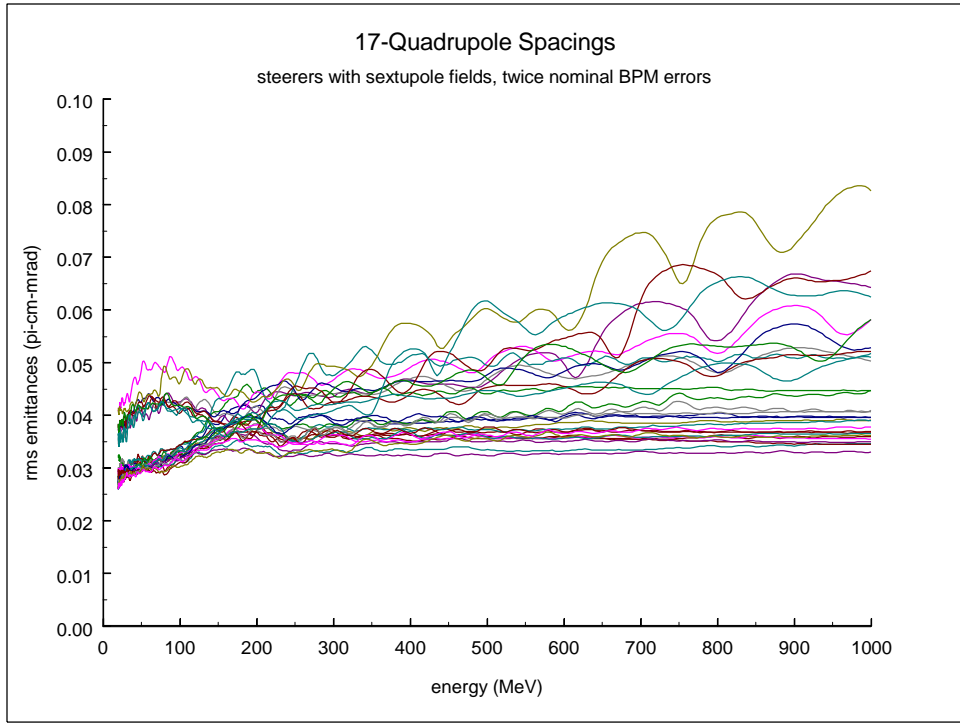


Figure 41. Steering scheme with 17-quadrupole spacings, twice nominal BPM errors.

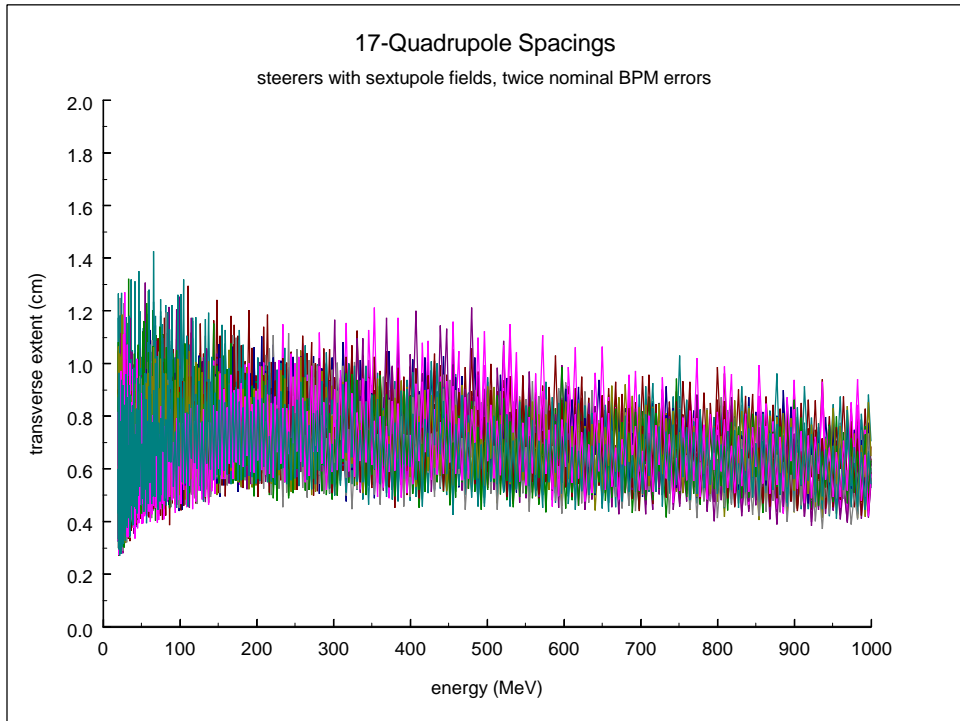


Figure 42. Steering scheme with 17-quadrupole spacings, twice nominal BPM errors.

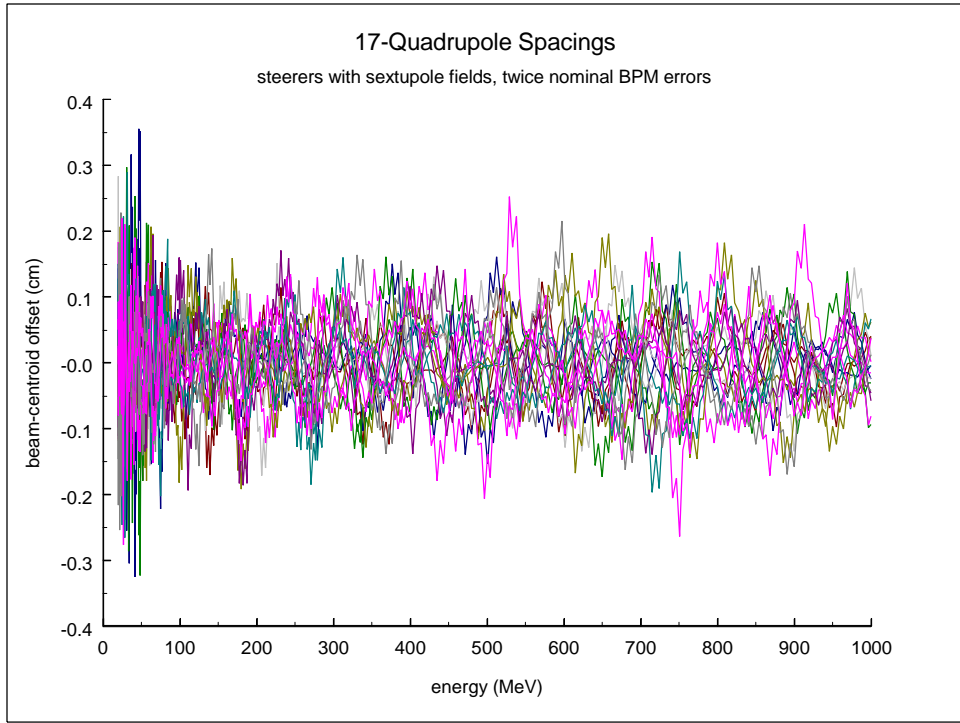


Figure 43. Steering scheme with 17-quadrupole spacings, twice nominal BPM errors.

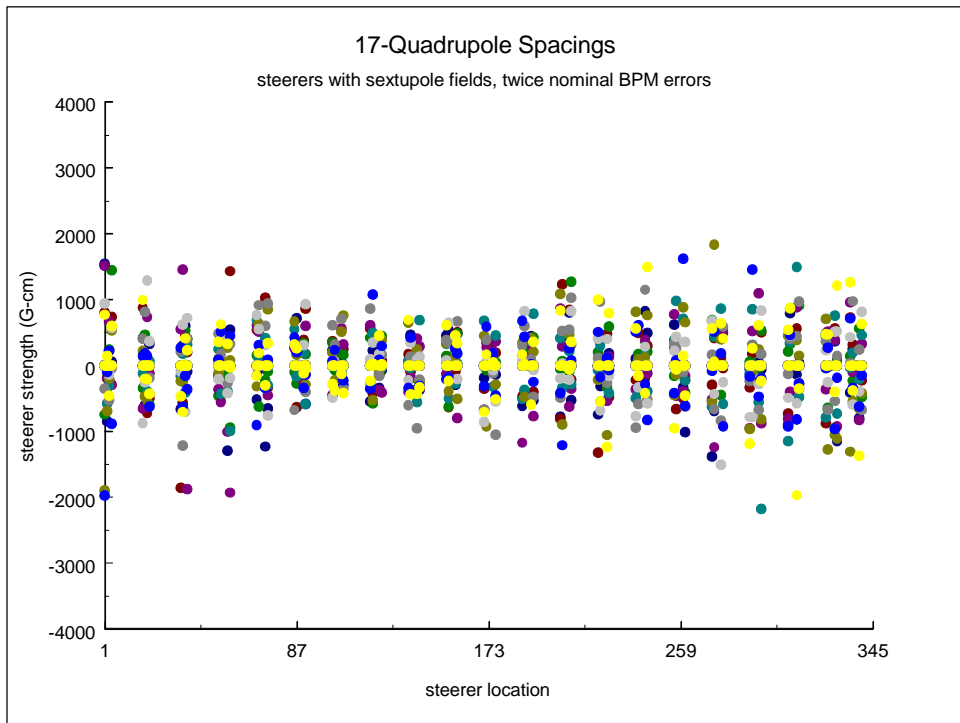


Figure 44. Steering scheme with 17-quadrupole spacings, twice nominal BPM errors.

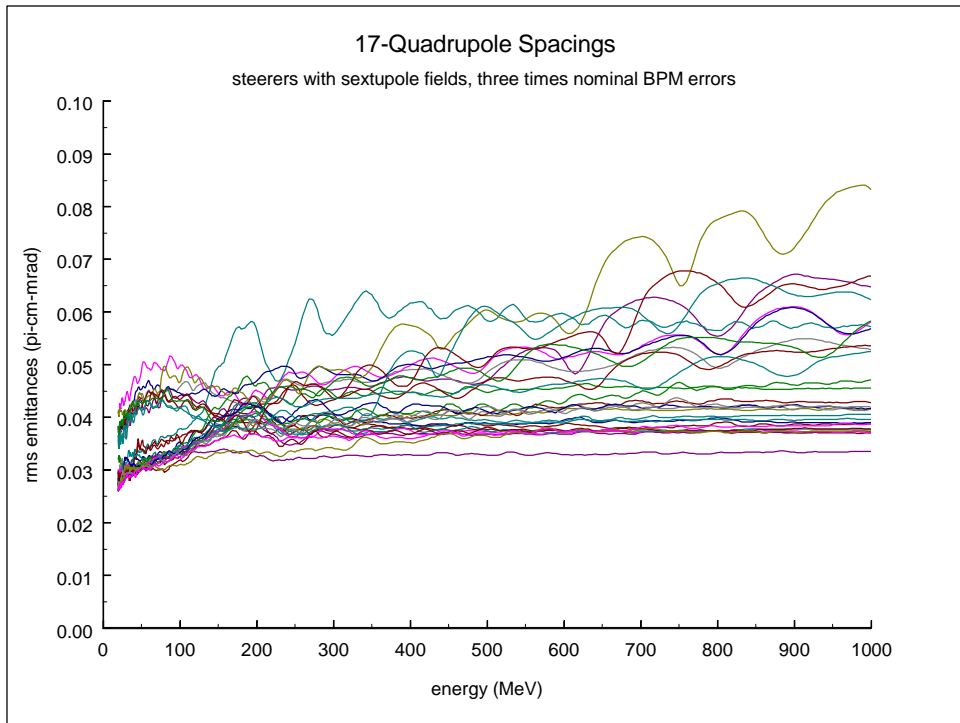


Figure 45. Steering scheme with 17-quadrupole spacings, three times nominal BPM errors.

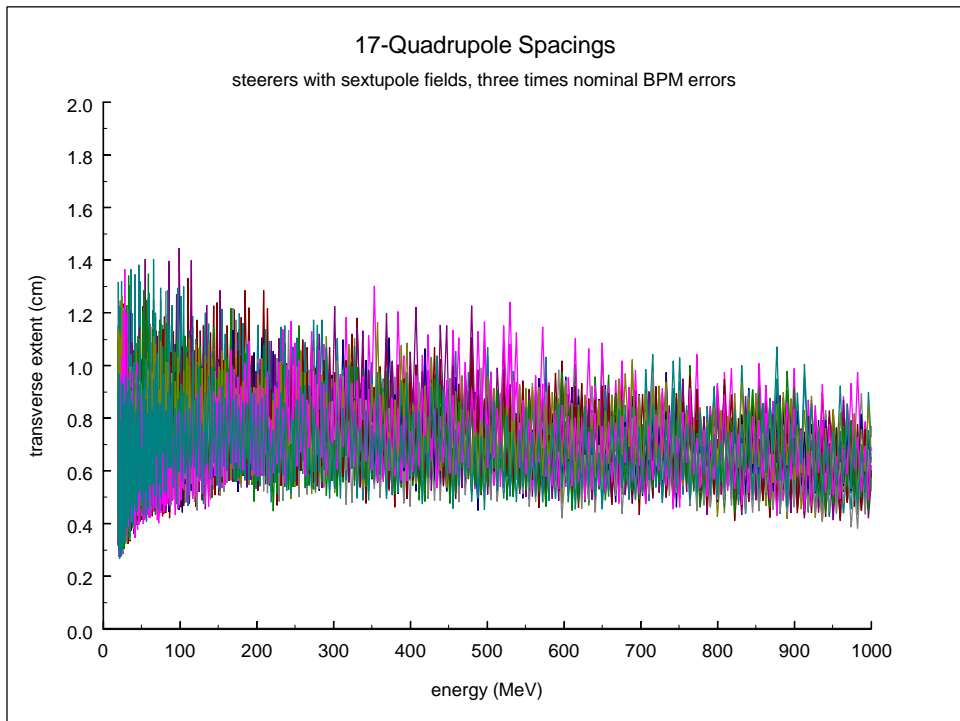


Figure 46. Steering scheme with 17-quadrupole spacings, three times nominal BPM errors.

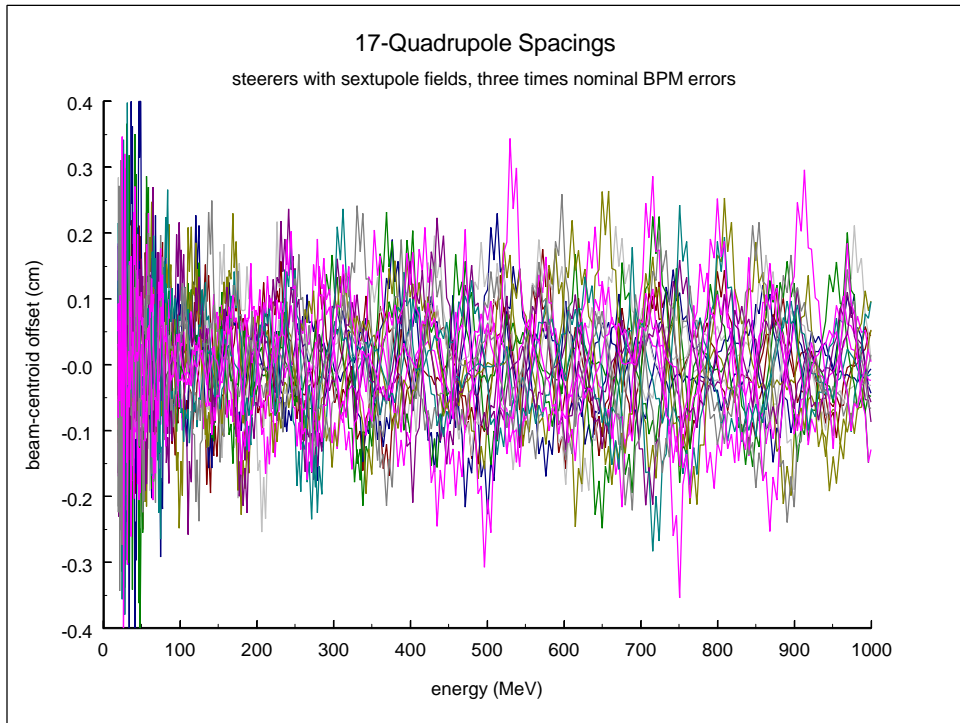


Figure 47. Steering scheme with 17-quadrupole spacings, three times nominal BPM errors.

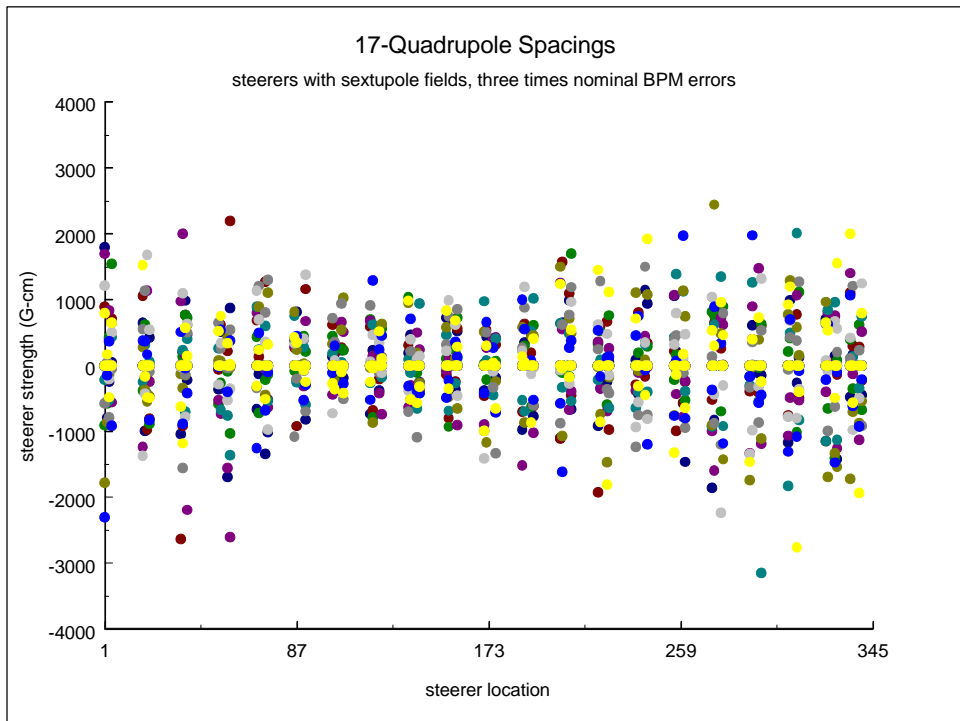


Figure 48. Steering scheme with 17-quadrupole spacings, three times nominal BPM errors.

